Simultaneous measurement of labile U(VI) concentration and (234U/238U) activity ratio using a Monophos®-based Diffusive Gradients in Thin-films sampler.

Josselin Gorny, Charlotte Lafont, Clémentine Sapey, Steffen Happel, Alkiviadis Gourgiotis, Laureline Fevrier, Josep Galceran

Journal Pre-proof

Simultaneous measurement of labile U(VI) concentration and ($^{234}U/^{238}U$) activity ratio using a Monophos®-based Diffusive Gradients in Thin-films sampler.

Josselin Gorny, Charlotte Lafont, Clémentine Sapey, Steffen Happel, Alkiviadis Gourgiotis, Laureline Février, Josep Galceran

PII: S0003-2670(24)01067-5

DOI: https://doi.org/10.1016/j.aca.2024.343266

Reference: ACA 343266

To appear in: *Analytica Chimica Acta*

Received Date: 8 April 2024

Revised Date: 18 September 2024

Accepted Date: 19 September 2024

Please cite this article as: J. Gorny, C. Lafont, C. Sapey, S. Happel, A. Gourgiotis, L. Février, J. Galceran, Simultaneous measurement of labile U(VI) concentration and ($^{234}U/^{238}U$) activity ratio using a Monophos®-based Diffusive Gradients in Thin-films sampler., *Analytica Chimica Acta*, https://doi.org/10.1016/j.aca.2024.343266.

Graphical abstract:

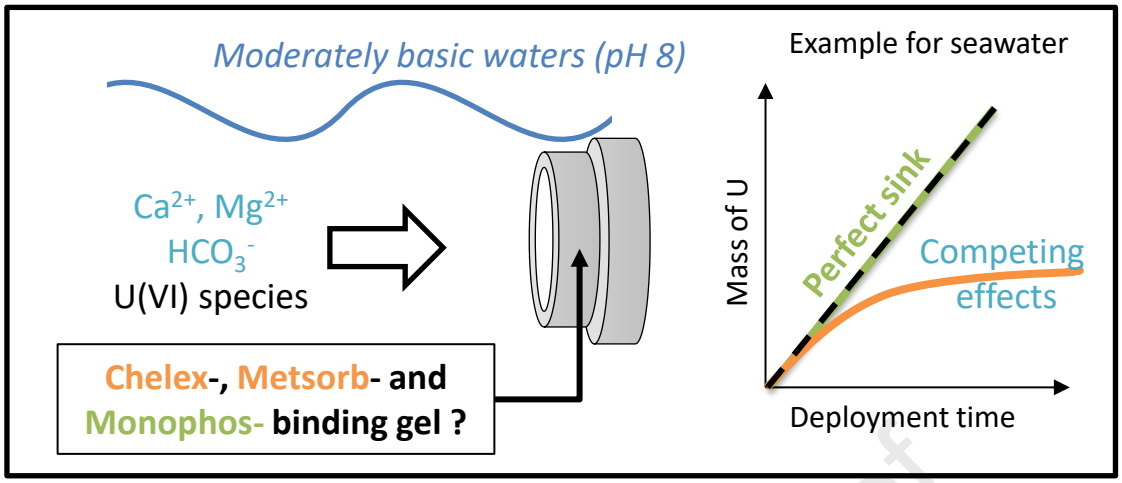

Simultaneous measurement of labile U(VI) concentration and ($^{234}U/^{238}U$) activity ratio using a Monophos®-based Diffusive Gradients in Thin-films sampler.

Josselin Gorny[a*], Charlotte Lafont[a], Clémentine Sapey[a], Steffen Happel[b], Alkiviadis Gourgiotis[a], Laureline Février[c], Josep Galceran[d]

[a] Institut de Radioprotection et de Sûreté Nucléaire (IRSN), PSE-ENV/SPDR/LT2S, F-92260, Fontenay-aux-Roses, France

[b] TrisKem International, Bruz, France

[c] Institut de Radioprotection et de Sûreté Nucléaire (IRSN), PSE-ENV/SPDR/LT2S, F-13115, Saint Paul-lez-Durance, France

[d] Departament de Química, Física i Ciències Ambientals i del Sòl, Universitat de Lleida and AGROTECNIO-CERCA, Rovira Roure 191, 25198, Lleida, Spain

* Corresponding author: josselin.gorny@irsn.fr

Keywords:

Uranium; Diffusive Gradients in Thin-films; Inorganic speciation; Laboratory validation; intercomparison; field application

Abstract

Background: In a context of environmental monitoring around installations related to the nuclear fuel cycle, the Diffusive Gradient in Thin-films (DGT) technique captures the integrated concentration of U isotopes in their native environment, yielding comprehensive data on U origin (anthropogenic *vs* natural), total concentration, and mobility. However, for common deployment times (4-5 days) in moderately basic waters, none of the commercially available binding gels is adapted to measure the total U concentration. So, the development of novel DGT binding gels is timely.

Results: A new DGT sampler, using the Monophos® resin, as well as a new model for the interpretation of the DGT flux, has been successfully developed to measure the labile U concentration (which was also its total concentration) in moderately basic waters (pH ≈ 8). The model accounts for the penetration of uranyl carbonate complexes into the binding gel. Monophos-DGT samplers were able to quantify the total U concentration (accuracy >90 %) in three different mineral basic waters and in a synthetic seawater in laboratory experiments, as well as *in situ* in the

rivers Essonne and Œuf, France. Ion interferences (*e.g.*, Ca^{2+}, Mg^{2+} and HCO_3^-), critical when using Chelex and Metsorb resins as binding agents, were overcome by using the new DGT sampler, thus allowing for a longer linear accumulation of U in the tested matrices and, above all, a better detection of U minor isotopes improving the potential of using DGT samplers for water source tracing through isotopic measurements.

Significance: The use of the new DGT sampler and the new model for the interpretation of DGT flux is recommended to improve the accuracy of total U concentration determinations in field applications. Moreover, simultaneous elemental and isotopic measurements were successfully performed during field application, confirming new perspectives for environmental applications such as identification of U pollution sources by using isotopic signatures.

1. Introduction

Uranium (U) presents a unique challenge for ecological risk assessments around installations related to the nuclear fuel cycle, because of its chemical and radiological toxicity. Their relative importance depends on the chemical speciation and on isotopic composition of the radioelement, the latter being strongly correlated to its natural or anthropogenic origin (enriched or depleted U) [1]. In this framework, the Diffusive Gradient in Thin-films (DGT) technique is an appealing tool for monitoring water quality around U processing plants, nuclear facilities or mining areas as illustrated in the literature [2-10]. The standard configuration of DGT samplers consists of a binding disc (or "resin"), a thin diffusive gel disc and a filter. DGT samplers preconcentrate U(VI) species *in situ*, allowing one to simultaneously characterize the labile UO_2^{2+} fraction in water and the isotopic composition at trace levels, as illustrated in reference [10] with ($^{235}U/^{238}U$) ratio.

A short overview on more than 20 years of work is made here to quickly explain the current status of the study, and we recommend the review of Pantoja and co-workers [11] for additional information. The community of DGT developers/users has been very active with U, as shown in Table 1. DGT developments and/or applications are generally focused on waters, and the most employed binding phases are Chelex®-100 resin (a cation-exchange resin with iminodiacetic acid functional groups; hereafter "Chelex"), Metsorb™ HMRP 50 sorbent (an agglomerated nanocrystalline titanium dioxide adsorbent; hereafter "Metsorb") and Diphonix® resin (a cation-exchange resin with carboxylic, diphosphonic and sulfonic acid functional groups; hereafter

"Diphonix") probably due to their commercial availability. According to comparative studies [12-16], the Diphonix-DGT samplers have a better performance than Chelex- and Metsorb-DGT samplers to measure all U species (total concentration). Diphonix-DGT method is indeed very slightly impacted by the common aqueous species found in environmental waters *e.g.*, Ca^{2+}, Mg^{2+}, SO_4^{2-} and PO_4^{3-}. So, its application is possible in surface waters with very different physico-chemical compositions, as recently shown by Smolíkova *et al.* [12] along the Scheldt estuary (Belgium). However, the Diphonix® resin is no longer marketed by Triskem International (https://www.triskem-international.com/), thus rendering progressively impossible to use Diphonix-DGT samplers.

In this study, we have, consequently, investigated the possibility of developing a DGT using a new binding gel proposed by Triskem International: the Monophos® resin (a cation-exchange resin with monophosphonic acid and sulfonic acid functional groups; hereafter referred to as "Monophos"). This study focused on assessing the performance of the new DGT sampler in moderately basic waters (pH ≈ 8) for which solution speciation of U is dominated by carbonate complexes [17, 18]. More specifically, our first objective was to propose a new experimental validation scheme, combining three types of DGT experiments (time-series experiment, apparent diffusive boundary layer experiment and double resin experiment), to better understand the behaviour of U species (*i.e.*, free uranyl and carbonates species) inside the DGT sampler and develop a suitable model to interpret the DGT flux. The second objective was to check whether the Monophos-DGT uptake of U was impacted or not by changes in the ionic strength, and to compare its performances to Chelex- and Metsorb-DGTs. The third objective was to establish the performances of the various DGT samplers (Chelex, Metsorb and Monophos) in different matrices in the lab, with special emphasis given to natural waters (two mineral waters and a synthetic seawater) and to the impact of possible interferences from the most relevant major species (*i.e.*, Ca^{2+}, Mg^{2+}, HCO_3^- and SO_4^{2-}). The fourth objective consisted in the *in situ* application of the DGT samplers (Chelex, Metsorb and/or Monophos) in two French rivers where the potential of using these DGT samplers for U source tracing through isotopic measurements was also assessed. Figure 1 schematically illustrates some contributions of this work. Notice the novelty of conducting dedicated experiments (see inside the dashed line in its panel A and D) to define (and develop) the best interpretative model.

2. Experimental section

2.1 Reagents and solutions

All solutions were prepared with deionized water (18.2 MΩ cm^{-1} resistivity, Milli-Q water, Millipore). High purity acids were obtained by distillation (Savillex® DST-1000 system) from HCl (Merck, Emsure 37 %) and HNO_3 (VWR Chemicals, Normapur 68 %). The following chemicals were used: agarose (Bio-rad), ammonium persulphate (Merck, electrophoresis), $CaCl_2.H_2O$ (Merck, pro analysis), Chelex®-100 (sodium form, 200-400 mesh, Bio-Rad), (1-Hydroxyethan-1,1-diyl)bis(phosphonic acid) (hereafter "HEPDA", Alfa Aesar, 96 %), H_2O_2 solution (30 %, VWR, Analar Normapur), Metsorb® HMRP 50 (Graver technologies, Glasgow, DE, USA), Monophos® (proton form, 100-200 mesh, Triskem international), UTEVA® resin (100-150 µm, Triskem International), N,N,N′,N′-tetramethylethylenediamine solution (99%, Merck, GR for analysis), Na_2CO_3 (VWR Chemicals, Analar Normapur) and NaCl (Merck, suprapur). The following salts provided from VWR Chemicals (all with Analar Normapur quality): $MgCl_2.6H_2O$, NaCl, $NaHCO_3$, $NaNO_3$ and Na_2SO_4. The following standard solutions were used: U standard solution employed to spike the deployment solution (1 g L^{-1}, matrix 2 % HNO_3, CPAChem, natural isotopic composition), the IRMM 3636 solution reference material (solution for certified for $^{233}U/^{236}U$ isotope ratio), multi-element standard solution VIII (24 elements, 100 mg L^{-1}, matrix 6 % HNO_3, Supelco, Certipur®) and anion chromatography standard solution including Cl^-, Br^-, NO_3^-, NO_2^-, SO_4^{2-} and PO_4^{3-} (100 mg L^{-1}; matrix deionized water, CPAChem).

2.2 Materials and equipment

Two polycarbonate containers (395 × 340 × 305 mm) were custom-made by Star Pack (https://www.star-pack.fr/); polycarbonate is indeed known to be relatively more inert to U(VI) species compared to polypropylene [15, 19, 20]. These polycarbonate containers were acid-cleaned in 1.5 mol L^{-1} HNO_3 solution over 24 h, then rinsed several times with deionized water prior to the deployment in them of the DGT samplers. For the deployment, a Perspex® DS24 holder (DGT Research Ltd) equipped with a maximum of twelve DGT samplers was placed horizontally in the centre of the polycarbonate container. Three Perspex® sheets were used to lock the Perspex® DS24 holder, and these ones could be removed quickly and easily during time-series experiments. The deployment solutions were stirred using a Bioblock scientific 74402 orbital shaker (250 rpm).

2.3 General DGT procedures and uranium analysis

Agarose (AGE) hydrogels were selected as standard diffusive gels [21]. They were made in our laboratory, with their thicknesses (300, 400, 500 and 800 µm) controlled using an optical microscope. They were stored in 10 mmol L^{-1} NaCl solution (made from ultrapure salt). Chelex- and Metsorb-binding gels were routinely prepared following the procedure described by Zhang & Davison [22] and Bennett and co-workers [23], respectively. The thickness of Chelex- and Metsorb-binding gel was 480 µm. Contrary to other binding gels (where agarose-polyacrylamide, APA, is the matrix), AGE hydrogel was also employed as structural material to make the Monophos-binding gel. Briefly, 2 g of wet Monophos-resin beads (moisture content of 53.4 %) were mixed with 10 mL of 1.5 % hot agarose solution. These mixtures were, then, inserted between two acid-cleaned hot glass plates (45°C) separated by an 800-µm polytetrafluoroethylene plastic spacer and left at room temperature for at least 30 min. The Monophos-binding gel plate surface varied between 100 and 120 cm^2. Once the Monophos-binding gels were completely polymerized, they were separated from the glass plates, rinsed several times to remove unreacted reagents with ultrapure water (24 h) and stored into 10 mmol L^{-1} NaCl bath (made from ultrapure salt). Note that the use of two layers (*i.e.*, diffusive and binding gels) using AGE instead of carcinogenic APA as hydrogel significantly reduces costs, simplifies the manufacturing process and most importantly meets internal requirements to progressively reduce the exposition of hazardous materials. The binding gel (either 480 or 800 µm-thick), the AGE diffusive gel (300 to 800 µm-thick) and the polyethersulfone filter membrane disc (140 µm-thick, 0.45 µm pore size, Pall) were assembled in a piston-type acrylonitrile butadiene styrene DGT holder with a sampling area of 3.14 cm^2 (DGT Research Ltd). When the 300 µm-thick AGE diffusive gel was employed in the DGT sampler, a polytetrafluoroethylene disc was used to compensate the empty space under the Monophos-binding gel. Assembled DGT samplers were stored at 4°C in doubled zip-lock plastic bags, which contained a small amount of 10 mmol L^{-1} NaCl solution (made from ultrapure salt) to maintain the moisture. Following the retrieval of the DGT samplers after exposure, the binding gels were removed and eluted for 24 h with 3 mL of the selected eluent solution in a polypropylene tube (Section 4.1.1). In parallel, 10 mL of the deployment solution were collected and acidified at 300 mmol L^{-1} HNO_3. 4 mL of diluted eluent solution (at least 10-fold diluted using 300 mmol L^{-1} HNO_3 solution) or 4 mL of acidified deployment solution were mixed with 10 µL of IRMM 3636 double spike with a $^{233}U/^{236}U$ isotope ratio of 1:1 and an initial ^{236}U concentration at 8.67 ng g^{-1} for U analysis. In this

work, all U isotope measurements were performed using an Agilent 8800 ICP-MS/MS (Agilent Technologies, Tokyo, Japan) located at the IRSN's PATERSON platform [24]. The ICP-MS/MS was run in single quadrupole mode (hereafter referred to as ICP-MS). The ICP-MS operating conditions can be found in Table S1 in the Supporting Information file. ^{235}U concentration was measured by isotope dilution through the $^{235}U/^{236}U$ ratio and, then, the ^{238}U concentration (hereafter "U") was calculated by taking into account the natural $^{238}U/^{235}U$ ratio (137.818±0.045) [25]. Similarly, the ($^{234}U/^{238}U$) activity ratio was calculated from the $^{234}U/^{235}U$ ratio and converted to $^{234}U/^{238}U$ using the natural $^{238}U/^{235}U$ ratio and, then, into the activity ratio using the ^{234}U and ^{238}U half-lives. It should be noted that before calculating the ($^{234}U/^{238}U$) activity ratio, controls were carried out to ensure that the $^{238}U/^{235}U$ isotope ratio is the natural one in the surface waters of the Œuf and the Essonne rivers, France.

For all isotope ratios, the instrumental mass bias was corrected using the exponential mass fractionation law [26] by taking into account the reference value of the $^{233}U/^{236}U$ of the IRMM 3636. $^{234}U^{+}$ signal was corrected for ^{233}U hydride contribution ($^{233}UH^{+}$) by measuring the signal at m/z =239 ($^{238}UH^{+}$) and for the ^{234}U spike impurities ($^{234}U/^{236}U$ = 0.000366). To assess the precision and accuracy of our measurements, we prepared solutions from Harwell Uraninite (HU-1) that is known to be close to secular equilibrium with respect to $^{234}U/^{238}U = 54.887\times10^{-6}$ [27]. Finally, the accumulated mass of U(VI) species by DGT samplers (M_{DGT}, *e.g.* in pmol) was calculated using

$$M_{DGT} = \frac{c_e(v_e + v_{gel})}{(f_e/100)} \quad (1)$$

where c_e is the eluted concentration of U in the selected elution solution (*e.g.*, in pmol mL^{-1}), v_e the eluent volume (mL), v_{gel} the volume of binding gel (mL) and f_e the elution factor (%).

2.4 Laboratory experiments

2.4.1 Selection of the binding gel elution solution

The following strategy (which assumes full reversibility of the adsorption/desorption process) was implemented to select the appropriate eluent. The binding gels were immerged for 24 h in 3 mL of HNO_3, HEDPA or HNO_3/H_2O_2 solution (all at 1 mol L^{-1}) containing 420 nmol L^{-1} of U. The elution factor (f_e, %) in each immersion solution was calculated using

$$f_e = \frac{M_f}{M_i} \times 100 \quad (2)$$

where M_i and M_f are, respectively, the initial and final mass of U in the immersion solution. Batch experiments were performed at room temperature (20±2°C).

As the amount of Ca^{2+} and Mg^{2+} accumulated by the binding gels will be determined along the time-series experiment in complex matrices (Section 4.1.7), the adsorption of these alkaline earth metals was tested as described above , with HNO_3 or HEDPA solution (1 mol L^{-1}) containing Ca^{2+} and Mg^{2+} at 0.25 mmol L^{-1}.

2.4.2 Time-series experiments in simple matrices and Volvic® water

Time-series experiments were performed to verify the linear response of the Monophos-based binding gel. After preparing 8 L of deployment solution spiked at around 84 nmol L^{-1} U, a Perspex® DS24 holder was placed inside the polycarbonate container. To test the effect of U speciation on the DGT uptake, two deployment solutions were used: (i) 10 mmol L^{-1} $NaNO_3$ at pH 3 (pH adjusted with 15 mol L^{-1} HNO_3 solution); (ii) a mixture of 10 mmol L^{-1} $NaNO_3$ and 1 mmol L^{-1} $NaHCO_3$; and (iii) Volvic® water (selected as "natural water model"). The addition of bicarbonate buffers the pH of the second deployment solution to 8.0 ± 0.3, and it also stabilizes U in the deployment solution by forming carbonate complexes [13]. After equilibration of the deployment solution with the atmosphere during at least 24 hours, twelve Monophos-DGT samplers were simultaneously deployed. Then, three Monophos-DGT samplers were retrieved at specific time intervals (24, 48, 72 and 96 h).

2.4.3 Varying diffusion gel thickness experiments in simple matrices and Volvic® water

Monophos-DGT samplers equipped with three different thicknesses of AGE diffusive gel (300, 500 and 800 µm) were deployed for 24 h in the same matrices as above (section 2.4.2**)**. Four replicates of each thickness were used. The reciprocal mass of analyte (M_{DGT}^{-1}, $pmol^{-1}$) was plotted versus the thickness of the material diffusion layer (δ^{mdl}, cm). Two parameters will be obtained for the three waters: the effective diffusion coefficient and the apparent diffusive boundary layer (ADBL) [28, 29]. Calculations are presented in the sections 4.1.3 and 4.1.4, respectively.

2.4.4 Double resin experiments in simple matrices and Volvic® water

To check whether the Monophos-resin acts as a perfect sink, the DGT samplers equipped with a polyethersulfone filter (140 µm), an AGE diffusive gel (800 µm) and a stack of two Monophos-binding gel discs (2 × 800 µm) were prepared in four replicates. DGT caps with an opening window of 2.54 cm^2 were used for these experiments. To test the effect of U speciation on the possible penetration of U in the resin domain, the Monophos-DGT samplers were deployed for 24 h in the three deployment solutions presented above (Section 2.4.2). Calculation of the penetration length of U is discussed in Section 4.1.4.

The granulometric size distribution of Monophos-resin beads was determined using a Laser diffraction Particle Size analyser (Beckman Coulter LS 13 320) equipped with an Aqueous liquid module. Then, it was possible to compare the penetration length of U with the diameter of resin beads as previously performed [30, 31].

2.4.5 Effects of ionic strength on DGT performances

To evaluate the effect of ionic strength, triplicate Chelex-, Metsorb- and Monophos-DGT samplers were simultaneously deployed for 24 h in 8 L of deployment solution with varying concentrations of $NaNO_3$ (1, 10, 100 and 700 mol L^{-1}). These ionic strengths in the deployment solution were within the range of those encountered in the environment. As in the previous section, the deployment solutions were also doped with $NaHCO_3$ at 1 mmol L^{-1} and U at 84 nmol L^{-1}.

2.4.6 Time-series experiments in complex matrices

To determine the performances of each binding gel in environmentally relevant matrices, twelve DGT samplers containing either a Chelex-, a Metsorb- or a Monophos-binding gel were deployed in 8 L of Volvic®, Vittel® or synthetic seawater (prepared according to [32]). The deployment solutions were spiked with U at 84 nmol L^{-1}. All solutions were equilibrated with the atmosphere during at least 48 hours before DGT deployment. Their physico-chemical characteristics are reported in Table 2. Triplicate DGT samplers were removed after a defined deployment time (24, 48, 72 and 96 h). For DGT samplers deployed in seawater, before elution, each binding gel was immersed in 5 mL of ultrapure water for 4 h to remove unbound salts [15]. Measurement of total U concentration in the acidified synthetic seawater was performed after chemical extraction. Methodology is fully described in the supplementary data (Section S2).

To better understand the functioning of the DGT samplers for these time-series experiments, the amounts of Ca^{2+} and Mg^{2+} accumulated by the binding gels were also measured over time. Before elemental measurements, eluent solutions were diluted at least 10-fold using 300 mmol L^{-1} HNO_3 solution. Deployment solutions were also characterized. Methodology is fully described in the supplementary data (Section S1 and S2).

2.5 Field applications

Complementarily to the laboratory experiments, the Œuf river (Essonne, France) was selected to perform a field application. Its moderately basic surface waters are characterized by a high dissolved U concentration up to 84 nmol L^{-1}, but also by a ($^{234}U/^{238}U$) ratio varying from 1.1 to 0.41 with distance (from data in [33]**)**. Therefore, we used this site to test the suitability of the DGT samplers to measure the ($^{234}U/^{238}U$) ratio. The first field campaign was performed in February 2021. Three sampling points (SP), spaced by several kilometres apart, were selected along the Œuf river. Their respective GPS coordinates were: SP1: 48.09012”N, 2.18456”W; SP2: 48.16281”N, 2.24151”W; and SP3: 48.18603”N, 2.35193”W. At each sampling point, a Perplex® DS24 holder equipped with Chelex-, Metsorb-, and Monophos-DGT samplers (in triplicate) were horizontally placed at least 10 cm above the surface sediments, the filter surface being parallel to the flow of the river to get laminar conditions to minimize the diffusive boundary layer (DBL) length. The exposed surface area of DGT samplers was 3.14 cm^2. The deployment times of DGT samplers was 72h.

The second field campaign was performed in June 2023. The goal of this campaign was to assess the *in situ* applicability of the model that accounts for the penetration of U species in the resin domain of the Monophos-DGT samplers. Therefore, triplicate Monophos-DGT samplers equipped with 400-, 800- and 1600-µm thick diffusive gel (see Figure S4) and triplicate DGT samplers equipped with a stack of two 800 µm-thick binding gels as in Section 2.4.4 were deployed. The exposed surface area of DGT samplers was 2.54 cm^2. The sampling site SP4 was in the Essonne river, a tributary of Œuf river. Its GPS coordinates were: 48.50940”N, 2.36541”W. For this sampling point, a Perplex® DS12 equipped with the Monophos-DGT samplers was fixed horizontally on a rope at least 30 cm above the surface sediments. The deployment time of DGT samplers was 69 h.

For the two field campaigns, DGT blanks (in triplicate) were prepared along with the deployed DGT samplers and exposed to the field environment by opening the zip-lock bag during deployment and retrieval of the samplers. Field temperature was recorded every 10 min using a Tinytag temperature logger (TG-4100). In parallel to DGT deployment, numerous parameters were monitored in the dissolved fraction over time: major anion concentrations (Cl^-, NO_3^- and SO_4^{2-}), conductivity, dissolved organic carbon (DOC), dissolved inorganic carbon (DIC), pH, total elemental concentration (Ca, Mg, Na, K and U) and the ($^{234}U/^{238}U$) activity ratio. These parameters were obtained at 0, 24, 48 and 69/72 h. Methodology and analysis are fully described in the supplementary data (Section S1 and S2).

2.6 Chemical modelling

PHREEQC version 3.6.2.15100 (https://www.usgs.gov/software/phreeqc) was used to calculate the aqueous speciation of U(VI) in the different deployment solutions using the thermodynamic database PRODATA version 1.5.2 [34-36]. Input data are presented in Table 2. Equilibrium with atmospheric CO_2 and recorded pH and temperature were also used. Activity coefficients for the thermodynamic predictions were computed with the Davies equation for continental waters, while for synthetic seawater the specific ion interaction theory (SIT) equation was used.

3. Theoretical model for penetrating labile species into the resin domain

A suitable model, that accounts for the penetration of the U labile species into the resin domain, has been developed to interpret the results. It assumes the following hypotheses: a) Uranyl (UO_2^{2+}) and its complexes (*e.g.*, uranyl-carbonate complexes) penetrate into the binding layer; b) All complexes are fully labile; c) Ligands are in excess with respect to uranyl (with no relevant concentration differences between diffusion domains); d) The binding disc capacity is much larger than the actual occupation of sites (*i.e.*, excess conditions for the resin); d) There is no desorption of uranyl species, once they are bound to the resin; e) The system is in steady state; and d) Electrostatic effects between resin phase and diffusive gel phase are negligible.

Due to the full lability of the complexes, it is convenient to define average diffusion coefficients (denoted with an overbar) for each of the diffusion domains or phases (resin phase, sample solution, etc.):

$$\bar{D}^{phase} = \frac{D^{phase}_{UO_2^{2+}}\left[UO_2^{2+}\right] + D^{phase}_{UO_2CO_3}\left[UO_2CO_3\right] + D^{phase}_{UO_2(CO_3)_3^{2-}}\left[UO_2(CO_3)_3^{2-}\right] + \ldots}{c_{T,U}} \quad (3)$$

where $c_{T,U}$ represents the total concentration of U measured by ICP-MS in the considered deployment solution (with its own bulk speciation $\left[UO_2^{2+}\right], \left[UO_2CO_3\right], \left[UO_2(CO_3)_3^{2-}\right], \ldots$).

The derivation of the model follows the steps of Levy *et al.* [30, 37] by adapting a few parameters. See details in the Section S3. The penetration length (λ_{labile}) now becomes:

$$\lambda_{labile} = \sqrt{\frac{\bar{D}^{R}}{\bar{k}'_{a,R}}} \quad (4)$$

where the superscript "R" indicates the binding material (resin) phase, $\bar{k}'_{a,R}$ is the (excess) average association rate constant between the binding material and each of the uranyl species (in s^{-1}). The subscript "M" that appeared for λ in Levy *et al.* [37] has been changed to "labile" in order to highlight that the parameter applies to an ensemble of labile species and not just to one free metal ion.

Parallel to eqn. 6 in [30] (or eqn. 5.27 in [38]), now, the ratio of expected accumulations in a stack of identical binding discs with a front and a back disc is

$$\frac{n^{f}}{n^{b}} = 2\cosh\left(\frac{\delta^{r}}{2\,\lambda_{labile}}\right) - 1 \quad (5)$$

where δ^{r} indicates the aggregated thickness of both resin discs.

As detailed in the Section S3, and following the steps in the derivation of eqn. 7 in [31] (with no electrostatic factor), for a DGT device with any number of resin discs, the expected theoretical mass can be computed as:

$$M_{th} = At\,\frac{c_{T,U}}{\frac{\delta^{dbl}}{\bar{D}^{w}} + \frac{\delta^{mdl}}{\bar{D}^{mdl}} + \frac{\lambda_{labile}}{\bar{D}^{R}}\coth\left(\frac{\delta^{r}}{\lambda_{labile}}\right)} \quad (6)$$

where superscripts "w", "mdl" and "R" indicate, respectively, the diffusion domain in the phases: diffusion boundary layer, the material diffusion layer (diffusive gel + filter) and the resin. A is the

physical geometrical area of the DGT device window (2.54 or 3.14 cm^2) and t the deployment time of DGT sampler (in s).

To confirm, during laboratory experiments, that the DGT samplers are able to quantitatively measure the total U concentration in deployment solution, M_{DGT}/M_{th} accuracy value must be equal to 100 ± 15% as in our previous DGT developments [31, 39-41]. Equivalent to M_{DGT}/M_{th} is the ratio $c_{T,U,DGT}/c_{T,U}$, where $c_{T,U,DGT}$ is the total U concentration obtained from eqn. (6) (*i.e.* solving for $c_{T,U}$) with DGT experimental data and $c_{T,U}$ is the total concentration in the deployment solution measured by ICP-MS.

4. Results and discussion

4.1 Laboratory validation

4.1.1 Selection of the binding gel eluent solution

To define the eluent solution, the adsorption of U to Chelex-, Metsorb- or Monophos-binding gels was tested using 3 mL of either HNO_3, HNO_3/H_2O_2 or HEDPA solution (all at 1 mol L^{-1}). Note that there was no adsorption of U onto the walls of the polypropylene tubes when using these matrices. Results are displayed in Figure 2. A relevant U adsorption on the Monophos-binding gel was obtained in HNO_3 and HNO_3/H_2O_2 solution ($f_e \leq 15\ \%$), whereas the use of HEPDA solution prevents U adsorption on the resin ($f_e = 103.5 \pm 2.0\ \%$). At the opposite, no adsorption of U on either Chelex or Metsorb binding gels was obtained for the three solutions ($f_e = 97 - 102\ \%$). From these results, f_e can be set to 100% when calculating the accumulated mass of U by Chelex- and Metsorb-binding gels, as well as for Monophos-binding gel using HEDPA solution.

Previously reported f_e values were 83.2–96.2 and 63–79.5 % for Chelex- and Metsorb-binding gel using 1 mol L^{-1} HNO_3 solution, respectively [13, 15, 29, 42-44]. Other f_e values have been also obtained for Metsorb-binding gel using 1 mol L^{-1} HNO_3/H_2O_2 solution ($f_e = 83.0 - 83.2\ \%$), 1 mol L^{-1} Na_2CO_3/H_2O_2 ($f_e = 70.0 - 88.7\ \%$) and 1 mol L^{-1} $NaOH/H_2O_2$ ($f_e = 95.2 - 98.4\ \%$) [15, 20].

Contrary to this study, low elution efficiencies for Metsorb-binding gel were reported [45, 46] using 1 mol L^{-1} HNO_3 and 1 mol L^{-1} HNO_3/H_2O_2 solutions. From our results, there are several options to totally elute U from Chelex-, and Metsorb-binding gel. HNO_3 solution was selected as elution agent. Indeed, the addition of H_2O_2 implies no significant gain in elution efficiencies and it would also hinder analyzing U in a more complex matrix than HNO_3 solution (*i.e.*, the presence of H_2O_2 leads to the solubilization of Ti from Metsorb-binding gel disc in H_2O_2/HNO_3 solution [47]). HEDPA solution seems to be an alternative to HNO_3 solution. However, we have experimentally observed that dilute HEDPA solution in the plasma produces polymeric depositions on the ICP-MS cones. Similar difficulties have already been observed for phosphate-containing matrices, and even damage to the expensive cones has been reported [48-50]. Consequently, its use should be limited to the case of the elution of U from the Monophos-binding gel ($f_e = 100$ % for 3 mL of eluent).

The DGT blank values for U (evaluated using the selected elution procedure) were 0.4, 14.7 and 0.8 pmol for the Chelex-, Metsorb- and Monophos-DGT samplers, respectively. Even if our DGT blank values were slightly high compared to previous works (0.13-0.25 pmol for Chelex- and Metsorb-binding gels [16, 20]), they are low enough to determine the low total U concentration in environmental waters.

Concerning alkaline earth-metals, no adsorption was found for Ca^{2+} and Mg^{2+}: 100.3±5 and 104.2±4.6 % for Chelex binding gel; 99.0±5.7 and 104.9±4.6 % for Metsorb-binding gel; 88±2 and 89±2 % for Monophos-binding gel. From these results, still assuming the reversibility of adsorption/desorption of alkaline earth metals from the binding phase, f_e can set to 100% when calculating the accumulated mass of Ca^{2+} and Mg^{2+} for the Chelex- and Metsorb-binding gels. Concerning the Monophos-binding gel, the obtained f_e values for Ca^{2+} and Mg^{2+} were 88±2 and 89±3 %, respectively. The DGT blank values for Ca^{2+} and Mg^{2+} were respectively: 2.0 and 1.4 nmol for Chelex-binding gel; 107.0 and 2.0 nmol for Metsorb-binding gel; 13.8 and 1.3 nmol for Monophos-binding gel. Previously reported f_e values for Ca^{2+} and Mg^{2+} were, respectively, 98.3±5.6% and 95.4±6.5% for Chelex-binding gel using 5 mL of 1 mol L^{-1} HNO_3 [51]. A similar result was obtained from our elution procedure, even if the volume employed was lower (3 mL).

To the best of our knowledge, no f_e values for alkaline earth elements had been reported previously for the Metsorb-binding gel.

4.1.2 Accumulation of U as a function of time for Monophos-DGTs in simple matrices and Volvic® water

Linear accumulation of U on Monophos-DGT was first checked with time-series deployments of DGT in two simple matrices at pH 3 and pH 8. U(VI) speciation is dominated by free uranyl (UO_2^{2+} >99%) in the first one, and by carbonate species ($UO_2(CO_3)_3^{4-}$ 60 % and $UO_2(CO_3)_2^{2-}$ 36 %) with a negligible fraction of free uranyl in the second one. Another DGT experiment was also run in Volvic® water to test the effect of other U carbonate species ($Ca_2UO_2(CO_3)_3$, $CaUO_2(CO_3)_3^{2-}$ and $MgUO_2(CO_3)_3^{2-}$) on the Monophos-DGT uptake. Their relative abundance is shown in Table 2.

In the experiments using Monophos-DGT samplers equipped with 800 µm-thick AGE diffusive gel removed at defined deployment times (Figure 3, panels A), good linear relationships were obtained between M_{DGT} and t ($R^2 > 0.95$). This relationship confirms the suitability of Monophos-binding gel for U.

4.1.3 Determination of the diffusion coefficient of U for Monophos-DGTs in simple matrices and Volvic® water

The diffusion coefficient of U in the material diffusive layer, $\bar{D}^{mdl}$, in simple matrices and in Volvic® water was determined from the experiments in which the Monophos-DGT samplers were equipped with three thicknesses of AGE diffusive gel (300, 500 and 800 µm). A linear plot of M_{DGT} reciprocal versus δ^{mdl} was observed ($R^2 > 0.95$; Figure 3, panels B), from which we calculated the $\bar{D}^{mdl}$ values for the three tested conditions.

To interpret the results, eqn. (6) is rewritten as

$$\frac{1}{M_{DGT}} = \frac{1}{Atc_{T,U}}\left(\frac{\delta^{dbl}}{\bar{D}^{w}} + \frac{\lambda_{labile}}{\bar{D}^{R}}\coth\left(\frac{\delta^{r}}{\lambda_{labile}}\right)\right) + \frac{1}{Atc_{T,U}\bar{D}^{mdl}}\delta^{mdl} = y + s\,\delta^{mdl} \quad (7)$$

From the slope s, $\bar{D}^{mdl}$ of 6.34±0.47, 6.24±0.26 and 4.63±0.10× 10^{-10} $m^2 s^{-1}$ at 25°C were found for the simple matrix at pH 3, the simple matrix at pH 8 and Volvic® water, respectively (Table 3). Notice that the obtained $\bar{D}^{mdl}$ value does not depend on the extent of diffusive boundary layer (δ^{dbl}) or on the penetration length (λ_{labile}). The $\bar{D}^{mdl}$ value for Volvic® is low compared to those obtained for simple matrices. One interpretation is a slower diffusion of $Ca_2UO_2(CO_3)_3$, $CaUO_2(CO_3)_3^2$ and $MgUO_2(CO_3)_3^{2-}$ in the material diffusion layer. The individual D values in water of UO_2^{2+}, $Ca_2UO_2(CO_3)_3$, $CaUO_2(CO_3)_3^{2-}$, $MgUO_2(CO_3)_3^{2-}$, $UO_2(CO_3)_3^{4-}$ and $UO_2(CO_3)_2^{2-}$, reported from potential-based molecular dynamics simulations, are the following: 7.66, 4.60, 5.06, 5.06, 5.52 and 5.52 × 10^{-10} m^2 s^{-1} at 25°C [52]. Using them and the relative abundance of U(VI) complexes (predicted by speciation calculations) in eqn. (3), the theoretical $\bar{D}^{mdl}$ values are 7.66, 5.47 and 4.74 × 10^{-10} m^2 s^{-1} at 25°C for the simple matrix at pH 3, the simple matrix at pH 8 and in Volvic® water. Overall, the good agreement between experimental and theoretical values of $\bar{D}^{mdl}$ lends further support to the assumption of full lability postulated in Section 3.

Our $\bar{D}^{mdl}$ values for simple matrices agree with the literature values, which range between 2.6 and 6.7 ×10^{-10} m^2 s^{-1} at 25°C (Table 3). The variability of reported $\bar{D}^{mdl}$ values could result from the various DGT components employed (indicated by the alphanumeric code in Table 3) in combination with the experimental conditions *i.e.*, solution composition and pH [13, 16], the reactivity of plastic containers [15, 19, 20, 29] and the theoretical framework employed to interpret DGT fluxes. These different combinations might induce changes in U(VI) speciation in the deployment solution and/or in transport behaviour of U(VI) species according to the material diffusion layer properties (*e.g.*, resistance, electrostatic or specific interaction effects) and/or changes in affinity and/or uptake kinetics [21, 53-56].

4.1.4 Double resin experiments and determination of the thickness of the diffusive boundary layer

Before running the double resin experiments, granulometric measurements of Monophos-resin beads were performed. The Monophos-resin beads have a size ranging between 69 and 147 µm (Figure S1), values in agreement with the product sheet (74-149 µm). In the case where λ_{labile} is

significantly higher than the median diameter of Monophos-resin beads (106 μm), penetration of U(VI) species into the resin domain will be concluded.

For experiments in the simple matrix at pH 3, in the simple matrix at pH 8 and in Volvic® water, the back resin disc accumulated around 0.7%, 1.1% and 0.3% of the front resin disc accumulation respectively, indicating that the resin does not act as perfect sink for uranyl. This very low back accumulation is consistent with a very strong binding material while the packed beads leave very small paths for percolation of the analyte. Also, the thicker the binding disc (800 μm in this case), the lower the back accumulation. From the quantities of U accumulated in the front and back resin discs and eqn. (5) and (4), we obtained λ_{labile} = 161.51±6.83, 170.77±12.39 and 139.69±0.66 μm ("minimum detectable λ_{labile}" being 116 – 121 μm, values estimated as in [37]), which are all superior to the median diameter of Monophos-resin beads (106 μm).

Applying the same equations, the mean association rate constants of U with the Monophos-resin were $\bar{k}'_{\text{a,R}} = 2.30\pm0.31$, 2.10 ± 0.39 and $2.32\pm0.07\times10^{-2}$ s^{-1} (values corrected at 25°C using Eqn. (4)) for experiments in the simple matrix at pH 3, in the simple matrix at pH 8 and in Volvic® water, respectively. As the $\bar{k}'_{\text{a,R}}$ values were not significantly different for the three deployment solutions, its average value ($\bar{k}'_{\text{a,R}} = 2.24\times10^{-2}$ s^{-1} at 25°C) was consequently employed to estimate M_{th}. Given the penetration found at pH 3, when no U complexes were present, we need to account for the penetration of the free uranyl in the resin domain to interpret our results. For experiments in the simple matrix at pH 8 and in Volvic® water, this assumption comes in addition to a possible penetration of other complexes of U. Equations expounded in Section 3 were applied to our results. Implicitly, this model was used by Turner [57].

From the ratio of intercept over slope (y/s) in eqn. (7), one can solve (parallel to eqn. 8 in [31]) for the thickness of the diffusive boundary layer (DBL)

$$\delta^{\text{dbl}} = \bar{D}^{\text{w}}\left(\frac{y}{\bar{D}^{\text{mdl}}s} - \frac{\lambda_{\text{labile}}}{\bar{D}^{\text{R}}}\coth\left(\frac{\delta^{r}}{\lambda_{\text{labile}}}\right)\right) \qquad (8)$$

With our data (see panels B in Figure 3), y/s yielded 258±70, 246±44 and 227±13 μm for experiments performed in the simple matrix at pH 3, in the simple matrix at pH 8 and in Volvic®

water, respectively. Then, we further assumed that the diffusion coefficients in the gel, filter and resin are equal to those for the same species in water, *i.e.*

$$\bar{D}^{\mathrm{mdl}} = \bar{D}^{\mathrm{R}} = \bar{D}^{\mathrm{w}} \equiv \bar{D}_{\mathrm{medium}} \tag{9}$$

where the subscript "medium" recalls that the average diffusion coefficient depends on each specific medium with a given composition of the sample (*i.e.*, percentages of free uranyl and of each of its complexes, see eqn. (3)). Under this assumption, eqn. (8) can be cast as

$$\mathrm{ADBL} \equiv \frac{y}{s} = \delta^{\mathrm{dbl}} + \lambda_{\mathrm{labile}} \coth\left(\frac{\delta^{\mathrm{r}}}{\lambda_{\mathrm{labile}}}\right) \tag{10}$$

Thus, from the calculated value of $\lambda_{\mathrm{labile}}$ for the temperature recorded during DGT deployment (eqn. (4)) and eqn. (8) , an average $\delta^{\mathrm{dbl}} = 86\ \mu\mathrm{m}$ (RSD = 5%, $n = 3$) for the three double-resin experiments was found. This δ^{dbl} seems acceptable for a vigorously stirred tank and was employed to estimate M_{th}. Note that, in the three deployment conditions, the penetration length is a non-negligible parameter even larger than the DBL length. After determining $\bar{D}^{\mathrm{mdl}}$ (Table 3), $\bar{k}'_{\mathrm{a,R}}$ and δ^{dbl} values for these three deployment conditions, we were able to satisfactorily reproduce, by using Eqn (6), the DGT response for the time-series experiments presented in panels A in Figure 3 ($M_{\mathrm{DGT}} / M_{\mathrm{th}} = 90.5 \pm 4.8\%$, 101.6±6.6% and 105.1±7.2% for experiments in the simple matrix at pH 3, in the simple matrix at pH 8 and in Volvic® water, respectively).

Notice that δ^{dbl} is seldom determined during DGT development as illustrated in Table 3, probably linked to the absence of commercial DGT caps able to safely accommodate various thicknesses of binding gel and diffusive gel layers.

4.1.5 Effects of ionic strength

The Monophos-DGT performances were tested in simple solutions with varying ionic strength ([$NaNO_3$] = 1-700 $mmol^{-1}$), and compared to the ones of Chelex-, Metsorb-DGT samplers. The pH of the deployment solutions for ionic strength tests was 8.0±0.3. Results are displayed in Figure 4. The DGT performances of the Monophos-binding gels were not influenced by ionic strength changes (up to 700 mmol L^{-1}), as well as the ones of Chelex- and Metsorb-binding gels. Indeed, acceptable $c_{\mathrm{T,U,DGT}} / c_{\mathrm{T,U}}$ ratios were obtained (94–111 %), where $c_{\mathrm{T,U}}$ stands for the total

concentration of U in the deployment solution measured with ICP-MS and $c_{T,U,DGT}$ is calculated with Eqn (6). This lack of ionic strength impact lends support to the hypothesis of no need of electrostatic factor in Eqn. (6) for similar conditions. Data obtained in all references commented next ([13, 15, 20, 29]) were obtained using DGT samplers equipped with an APA-based diffusive and binding gel disc, whereas ours were equipped with AGE diffusive gel disc. Hutchins and co-workers [15], using a model with DBL consideration, but without penetration of species into the resin, reported satisfactory DGT performances using Metsorb-binding gel for ionic strengths ≤ 10 mmol L^{-1} ($c_{T,U,DGT} / c_{T,U} = 100 \pm 4$ %), and significant underestimations at higher ionic strengths ($c_{T,U,DGT} / c_{T,U} = 82$ and 76 % for 100 and 700 mmol L^{-1} $NaNO_3$, respectively). In their experiments, the pH of the deployment solution was 8.0 ± 0.1. On the other hand, Drozdzak and co-workers [13], using a model without DBL consideration and without penetration of species into the resin, obtained different results: the Metsorb-DGT samplers were able to correctly estimate the total U concentration for ionic strengths up to 700 mmol L^{-1} ($c_{T,U,DGT} / c_{T,U} \sim 99-103$ %), whereas the response of Chelex-DGT samplers was good for ionic strengths up to 500 mmol L^{-1} ($c_{T,U,DGT} / c_{T,U} \sim 93-103$ %), and a low underestimation was observed at 700 mmol L^{-1} ($c_{T,U,DGT} / c_{T,U} = 81 \pm 4$ %). They observed no ionic strength effects on the Diphonix-DGT measurements ($c_{T,U,DGT} / c_{T,U} \sim 90-110$ %). In their experiments, the pH of the deployment solution was 7.0 ± 0.2. From batch experiments in which a binding gel disc was immerged in solutions with varying $NaNO_3$ concentrations (1–700 mmol L^{-1}) at pH 7, Turner and co-workers [20] found no appreciable impact of ionic strength on the uptake of U species by Chelex- and Metsorb-binding gel.

4.1.6 Performances of the Monophos-DGTs in complex matrices

After carrying out experiments in simple matrices and preliminary tests in Volvic® water (Sections 4.1.2, 4.1.3 and 4.1.4) the DGT performances of the binding gels were tested in two other complex matrices at pH 8.3 ± 0.3 (Vittel® water and a synthetic seawater). Long deployment times are often adequate to reveal possible interferences, and 72-96 h are typical deployment times for *in situ* investigations (to access low environmental concentrations). The complex matrices were especially selected to have a wide range of natural concentration of Ca^{2+} (0.39-13.6 mmol

L^{-1}), Mg^{2+} (0.44-114 mmol L^{-1}), HCO_3^- (1.03-2.38 mmol L^{-1}), Cl^- (0.22-675 mmol L^{-1}) and SO_4^{2-} (0.08-28.2 mmol L^{-1}). As the DGT samplers were not impacted by the ionic strength (section 4.1.5), non-linear accumulation, if any, should be the result of interferences present in the deployment solution. According to modelling, $Ca_2UO_2(CO_3)_3$ and $CaUO_2(CO_3)_3^{2-}$ were the two main U(VI) species in all waters except in seawater, in which two other supplementary U(VI) species are also present *i.e.*, $MgUO_2(CO_3)_3^{2-}$ and $UO_2(CO_3)_3^{4-}$ (see Table 2). The expected theoretical mass of U (M_{th}) that can be accumulated in the DGT samplers, assuming all U species are labile, has been computed with eqn. (6) and parameters in Table 3 and presented as the black continuous line in Figure 5). The "calibration parameters" obtained before for Volvic® waters (*i.e.*, $\overline{D}^{mdl} = 4.63 \times 10^{-10}$ m^2 s^{-1} at 25°C, $\overline{k}'_{a,R} = 2.24 \times 10^{-2}$ s^{-1} at 25°C and $\delta^{dbl} = 86$ µm) were used for the two other moderately basic waters due to the expected presence of similar U(VI) complexes (Table 2) and the proximity of the theoretical values of the diffusion coefficient in the three matrices (4.74, 4.78 and 5.08 × 10^{-10} m^2 s^{-1} at 25°C for Volvic®, Vittel® and synthetic seawater, respectively). When all experimentally measured mass accumulated in DGT (M_{DGT}) are between the dashed lines (which corresponds to an error of ±15% on the DGT measurement), one considers that there is a quantitative measurement of total U concentration by the DGT samplers. A $c_{T,U,DGT}$ not statistically different from $c_{T,U}$ is retrieved in eight of the nine plots for 24 h of deployment time (*i.e.*, time for which there is a limited competing effects) in Figure 5 by using eqns. (6) and (9). So, for the accepted tolerance level (±15%), the selected "calibration parameters" for Monophos are suitable for Vittel® water and synthetic seawater (panels B3 and C3, respectively). They seem also suitable for the two other binding materials except for Chelex in synthetic seawater.

For Volvic® and Vittel® waters (Figure 5, panels A3 and B3), good DGT responses were obtained using Monophos-binding gels, for the whole deployment time. The M_{DGT} points increased linearly up to 96 h ($R^2 > 0.95$), and all M_{DGT} points were included between the dashed lines ($M_{DGT}/M_{th} = 97.8$-101.6%). As the equilibration or saturation of the binding gels for U was not reached during these time-series experiments, the maximum safe deployment time could not be determined in these conditions, but it is clearly above 96h. Similar results were obtained for

Metsorb-DGT samplers (Figure 5, panels A2 and B2) *i.e.*, a linear accumulation of U and all M_{DGT} points were inside of the dashed lines (M_{DGT}/M_{th} = 104.6-105.3%) for the whole of deployment time. Consequently, since M_{DGT} matches M_{th}, the Monophos-DGT samplers can be suitable to measure $c_{T,U}$ in moderately basic continental waters with similar physico-chemical compositions, as well as Metsorb ones. Concerning the Chelex-DGT samplers, some M_{DGT} points were outside the dashed lines in Figure 5 A1 and B1 indicating poorer DGT performances. Linear accumulation of U was observed with Chelex-DGT samplers over time only for Volvic® waters (R^2 = 0.995), but the M_{DGT} points were globally 25 % under the M_{th} line. Signs of approach to equilibration of the Chelex-binding gel can be observed clearly for Vittel® waters. M_{DGT} points were below 1000 pmol for t > 24 h. The difference in DGT response in Volvic® and Vittel® waters could be attributed to competition effects presumably with Ca^{2+} [13, 20, 58] (~ 10 fold more concentrated in Vittel® waters) reducing the uptake of U(VI) species by Chelex-binding gel. In the case of Vittel® waters, as seen in the next section when discussing Figure S2, it is likely that Ca^{2+} ions displace U species previously bound to Chelex sites for deployment times longer than 50 h, so that the accumulation time-series goes through a maximum [59]. We conclude, by comparing with Metsorb- and Monophos-DGT samplers, that the Chelex-DGT samplers are less suitable to measure $c_{T,U}$ in moderately basic continental waters.

For the deployment in synthetic seawater, according to the experiments in $NaNO_3$ up 700 mmol L^{-1} (Figure 4), the response of the three DGT samplers is not expected to be impacted by the ionic strength. The linear regime was only obtained using the Monophos-binding gel (R^2 > 0.95), and all M_{DGT} points were included between the dashed lines as shown in Figure 5, panel C3 ($M_{DGT}/M_{th} = 110.2 \pm 4.3$ %). These results suggest that the Monophos-DGT samplers are suitable to measure $c_{T,U}$ in seawater. The Chelex- and Metsorb-DGT samplers underestimated $c_{T,U}$ for all deployment times ($M_{DGT}/M_{th} < 12\%$ and $< 87\%$, respectively; Figure 5, panels C1 and C2). Similar results were obtained for Chelex- and Metsorb-binding gel in previously reported time-series experiments in natural or artificial seawater, where different diffusive gels (than AGE) were used [12, 15, 20]. Our estimated effective capacities of these binding gels in seawater are around 1000 and 60 pmol for Metsorb-binding gel and Chelex-binding gel, respectively. The reduction of

uptake capacities in Chelex- and Metsorb-binding clearly reveals competition effects, in comparison to Monophos-binding gel. So, it is not recommended, for typical deployment times (72-96h), to employ the Chelex- or Metsorb-DGT binding gels to measure $c_{T,U}$ in seawater.

4.1.7 Interferences from Ca^{2+} and Mg^{2+}

To better understand the functioning of DGT binding phases, we also quantified the amount of Ca^{2+} and Mg^{2+} accumulated in the three binding gels as a function of time (Figure S2 and S3, respectively). From the time-series experiment, a linear accumulation of Ca^{2+} and Mg^{2+} up to 96h was only observed for Volvic® waters with Monophos-DGT samplers (R^2 = 0.9996 for the two elements; third column in Figure S2 and S3). This relationship could extend the suitability of using the Monophos-binding gel also for Ca^{2+} and Mg^{2+} determinations. The theoretical uptakes of Ca^{2+} and Mg^{2+} by Monophos-DGT samplers were computed by using Eqn (6) with their total concentrations given in Table 2, f_e obtained in Section 4.1.1, their respective $\bar{D}^w$ values (using the values for the free ions, 7.92 and 7.06 × 10^{-10} $m^2 s^{-1}$ at 25°C, respectively [60]) and $\bar{k}'_{a,R}$ = 2.24 ×10^{-2} s^{-1} at 25°C (*i.e.*, taking as a first approximation, the same parameter found for U). We were not able to satisfactorily reproduce the Monophos-DGT response for the time-series experiment in Volvic® water presented in Figure S2 and S3 (M_{DGT} / M_{th} = 115±5% and 117±5%, respectively). So, for a simultaneous Monophos-DGT measurement of Ca^{2+}, Mg^{2+} and U(VI) species it would be necessary to quantify specific calibration parameters (*e.g.*, $\bar{D}^{mdl}$ and $\bar{k}'_{a,R}$) for these alkali-earth metals in Volvic® water.

As shown in Figure S2 and S3, non-linear Ca^{2+} and Mg^{2+} accumulations were obtained for Vittel® water and for synthetic seawater. Signs of approach to equilibration or saturation for Ca^{2+} and Mg^{2+} were clearly observed with all M_{DGT} points being below the dashed lines ($M_{DGT} / M_{th} < 75\ \%$). From the results in synthetic seawater in the last column of Table S4, we can estimate a minimum value for the $Ca^{2+} + Mg^{2+}$ uptake capacity of Monophos-binding gel in the range 194-210 µeq, a value much higher than those presented thereafter for the Chelex- and Metsorb-binding gels. Comparing the theoretical uptake values estimated from the supplier (195-234 µeq), we conclude that equilibration of Monophos-binding gel was reached for Vittel® water

and for synthetic seawater. Although the Monophos-binding gel is not fully selective, its higher affinity for UO_2^{2+} (displacing Ca^{2+} and/or Mg^{2+}) and the relatively lower number of required sites for UO_2^{2+} binding seems sufficient to mostly avoid the interferences by Ca^{2+} and/or Mg^{2+}. This explains why no limitation of the uptake of U(VI) species by Monophos-DGT samplers for the three tested moderately basic waters up to 96 h was observed. Concerning the Chelex- and Metsorb-DGT samplers, M_{DGT} points in Figures S2 and S3 were below the M_{th} line (M_{DGT} / M_{th} 25 %). The amount of Ca^{2+} and Mg^{2+} did not evolve over time suggesting that equilibration/saturation was reached (RSD = 4-10 and 9-16 % for Chelex- and Metsorb-binding gel, respectively). In equilibrium (if one neglects competition effects), there is a direct proportionality between the accumulated amount and the concentration of the ion in the solution (in this case the total and the free concentrations of Ca^{2+} and Mg^{2+} are essentially the same). However, the found proportionality factor is not the same in Volvic® and Vittel® waters for a given DGT sampler. For instance, for Chelex-binding phase and Ca^{2+}, in Volvic® water, dividing the average accumulated amount of Ca^{2+} at 48, 72 and 96 hours (2.6 μmol in Table S4) by the total concentration in Ca^{2+} (0.39 mmol/L in Table 2) one obtains 6.67 mL. The same computation for Chelex-binding gel and Ca^{2+}, but in Vittel® water, yields 1.16 mL. Similar differences can be reached also for our results with Mg^{2+} (3.11 and 0.52 mL for Volvic® and Vittel® waters, respectively). The difference in the proportionality factors suggests that there is a relevant impact of competition in the binding of Ca^{2+} (due, for instance, to the uptake of Mg^{2+}) combined with an impact of the ionic strength. Conversely, the binding of Mg^{2+} would decrease in Vittel® waters with respect to Volvic® waters because of an increased amount of Ca^{2+} in Vittel and a larger ionic strength. These results agree with the observation, in a previous work [61], of a decreasing accumulation of Mg^{2+} with increasing ionic strength, justified in terms of changes in resin-association equilibrium and rate constants as well as a lower electrostatic partitioning. In conclusion, Ca^{2+} and Mg^{2+} can be interfering ions for U determination when Chelex-DGT samplers are deployed in synthetic seawater. In the last column of Table S4 for Chelex-DGT samplers, its total ion uptake was estimated using the total amounts of Ca^{2+} and Mg^{2+}.The similar total value (around 10.6 ± 0.9 μeq) obtained in Vittel® water and seawater, despite the different

Ca^{2+} / Mg^{2+} concentration levels of these two waters, suggests that this value is a good estimation of the effective uptake value of the Chelex-binding gel in these conditions. This value is close to the literature values ranging between 9 and 15 µeq [51, 62, 63]. These results confirm the conclusion formulated above *i.e.*, the uptake of U(VI) species by Chelex-DGT samplers is strongly impacted by Ca^{2+} and/or Mg^{2+} according to the deployment conditions. Furthermore, the accumulations of Ca^{2+} and Mg^{2+} on the Metsorb-binding gel reach equilibration, since all plots in Figures S3 and S4, central columns, stabilize in a plateau. However, as the total accumulations of Ca^{2+} and Mg^{2+} (5.1±0.7, 8.8±0.8 and 17.0±2.9 µeq for Volvic water, Vittel water and synthetic seawater, respectively; Table S4) still increase as a function of the deployment concentrations, it is not possible (as it was for the Chelex-binding gel) to confirm whether the effective uptake value has been reached. Nevertheless, for synthetic seawater, the reduction of the uptake capacity of U(VI) species in Metsorb-DGT sampler (see Figure 5) coincides with the higher accumulated amount of Ca^{2+} and Mg^{2+}. Data are not sufficient to elucidate the extent of Ca^{2+} and Mg^{2+} competition with the uptake of U(VI) species. This point will be further discussed in section 4.2.2.

4.2 Field applications

Two field applications were performed by deploying all types of DGT samplers in the Œuf river in 2021 (SP1, SP2 and SP3), and the Monophos-DGT samplers in the Essonne river in 2023 (SP4). Illustrations of DGT deployment are displayed in Figure 6 A and B. The deployment conditions and speciation calculation results for the two French rivers are summarized in Table 2. $c_{T,U}$ differed according to the sampling points (from 17 to 71 nmol L^{-1}). The field average temperature was 6.9±1.9, 9.8±1.0, 9.4±1.0 and 20.2±0.8°C for SP1, SP2, SP3 and SP4, respectively.

4.2.1 Field calibration

Experiments in the Essonne river (SP4) with only Monophos-binding gel and variable thicknesses of the diffusive gel layer led to a $\bar{D}^{mdl}$ of 4.35±0.31 ×10^{-10} m^2 s^{-1} at 25°C and $ADBL = y/s = 181 \pm 74 \mu m$ (data in Figure S4). This $\bar{D}^{mdl}$ value is in good agreement with laboratory values obtained in Volvic® waters, but also is consistent with the expected predominance of the two ternary complexes $Ca_2UO_2(CO_3)_3$ and $CaUO_2(CO_3)_3^{2-}$ (Table 2). Assuming eqn. (9) and eqn. (10) are valid, eqn. (6) can be re-written as

$$c_{\mathrm{T,U,DGT}} = \frac{M_{\mathrm{th}}}{\overline{D}^{\mathrm{mdl}} A t}\left(\mathrm{ADBL} + \delta^{\mathrm{mdl}}\right) \quad (11)$$

so that $c_{\mathrm{T,U,DGT}}$ can be computed for the two field applications in this section with no need of adopting any specific value for δ^{dbl} or for $\lambda_{\mathrm{labile}}$.

However, we have to report that our goal of simultaneously determining reliable specific values for δ^{dbl} and $\lambda_{\mathrm{labile}}$ in the Essonne river (SP4) could not be fulfilled. Indeed, experiments with two resins yielded a 9% back accumulation with respect to the total accumulation by the two binding gels, implying $\lambda_{\mathrm{labile}} = 323 \pm 12$ µm, which replaced in eqn. (10) would lead to a negative δ^{dbl}. So, these specific values of δ^{dbl} and $\lambda_{\mathrm{labile}}$ have not been used here.

As shown in Figure 6 C, where eqn. (11) was used with the ADBL value determined in the varying gel thickness experiments, the Monophos-DGT samplers were able to measure the total U concentration with a $c_{\mathrm{T,U,DGT}}/c_{\mathrm{T,U}}$ value of $102.5 \pm 1.2\%$.

Given the observed quasi-saturation of the resin with Ca^{2+} and Mg^{2+} in Vittel® water at 72 h and the reported high affinity of many metals (such as transition metals) for Monophos functional groups [64], we speculate that the back accumulation of U might have been overestimated perhaps be due to some displacement of U (initially attached to the front Monophos-binding layer) due to the composition of the river water. Further confirmation and rationalization of this unexpected high back-accumulation should be useful.

4.2.2 Field intercomparison

As the ionic strengths in the river sampling points are relatively close to that of Vittel® waters, we expected that only the Chelex-DGT response would be impacted by competition effects, presumably from Ca^{2+} and Mg^{2+} (Section 4.1.6), while Metsorb- and Monophos-DGT samplers would quantitatively measure the total U concentration. But, as illustrated in Figure 6 C (using the same parameters as in section 4.2.1), it was not totally the case: the Chelex- and Metsorb-DGT samplers accounted for just 4.0 to 7.1 and 19.0 to 27.3 % of the total U concentration, respectively, whereas the Monophos-DGT samplers were able to quantitively measure 92.4-107.9 % of $c_{\mathrm{T,U}}$. We speculate that the Metsorb-DGT underestimations might result from competition effects. Considering the total concentrations reported in Table 2, Ca^{2+} cannot be the main competitor in

these deployment conditions, because its concentration in the sampling points was very similar to its concentration in Vittel® water (where Metsorb-DGT sampler works well). The interference from Mg^{2+} can be discarded on similar grounds (higher concentration in Vittel® water than in the river). Another parameter not considered in the previous time-series experiments must be involved. Many experiments were performed with Metsorb-DGT samplers in [13, 20] to identify potential ion interferences (*i.e.*, Ca^{2+}, HCO_3^-, PO_4^{3-} and SO_4^{2-}), but most deployment conditions (pH 3.8-6.7) were unrepresentative of the moderately basic waters studied here and are not discussed here. In the study of Turner and co-workers [20], Metsorb-DGT samplers were deployed 24 h in a solution containing 10 mmol L^{-1} $NaNO_3$, variable concentration of $NaHCO_3$ (0.16-3.19 mmol L^{-1}) and 420 nmol L^{-1} U at pH 8.1±0.3. They observed that the Metsorb-DGT response became non-quantitative for [$NaHCO_3$] ≥ 1.5 mmol L^{-1} ($M_{DGT} / M_{th} = 20 - 70\%$). Therefore, in our case, the poor Metsorb-DGT response is likely to be mainly due to the high HCO_3^- concentration in the synthetic seawater and the surface waters of the Œuf river (~ 2 and 4-5 fold more concentrated than in Vittel® water). The Monophos-DGT samplers were consequently the most adapted to measure the total U concentration during this field application with $c_{T,U,DGT} / c_{T,U} \geq 92\%$. Compared to the Metsorb-binding gel, the Monophos-DGT response was not impacted by the presence of HCO_3^- up to 5 mmol L^{-1}. Therefore, in principle, there is no need to consider HCO_3^- as an interferent for the Monophos-DGT measurement.

($^{234}U/^{238}U$) activity ratio was also measured in this field application to ascertain whether the DGT technique could be used as a tool to identify the origin of U (either from natural background or coming from an industrial activity) or the source of waters (waters flowing through different geological bedrocks) as an alternative to the collection of spot water samples (Figure 6 D). A change in the ($^{234}U/^{238}U$) activity ratio from 0.97 to 0.42-0.45 along the Œuf river was well detected with both methodologies, without significant differences clearly pointing out that there is no significant isotope fractionation between ^{234}U and ^{238}U compared to the natural ($^{234}U/^{238}U$) variation (of the order of %) [65, 66]. Indeed, kinetic or equilibrium isotope fractionation for heavy isotopes is negligible compared to the heavy isotope ratio natural variations[67]. The ($^{234}U/^{238}U$) activity ratio precision obtained from the accumulation in the DGT sampler increased as follows: Chelex-binding gel (RSD = 4.8-13.9 %) < Metsorb-binding gel (RSD = 3.5-5.7 %) < Monophos-

binding gel (RSD = 1.9-2.4 %). These results are consistent because the larger the amount of U(VI) is accumulated by DGT samplers, the more the ($^{234}U/^{238}U$) activity ratio precision is improved. Another value (0.60) of ($^{234}U/^{238}U$) activity ratio was obtained with Monophos-DGT sampler in the Essonne river two years later. As expected, this one was not significantly different to the average of spot sampling (Figure 6 D).

5. Conclusions

A rigorous experimental design, combining three types of DGT experiments (Figure 1, panel A), was performed to assess the performances of a new DGT sampler (using the Monophos resin) for the measurement of U in moderately basic waters. Associated to the experimental tests, the development of a new model to interpret the U fluxes to the DGT accounted for the variation of the $\bar{D}^{mdl}$ values of U as a function of its speciation in the deployment solutions (see eqn. (3)), as well as for the small penetration of U species in the DGT-resin domain. Associated to the experimental tests, the development of a new model to interpret the U fluxes to the DGT accounted for the variation of the values of U as a function of its speciation in the deployment solutions (see eqn. (3)), as well as for the small penetration of U species in the DGT-resin domain. However, if one considers that the low percentages of back accumulation can be neglected, the interpretation of the results with the classical model (with no penetration, see section S4 in the Supporting Data) is slightly less accurate for the observed accumulations (see section S5) for this system.

The performance of Monophos-DGT to measure U in moderately basic waters (pH ≈ 8) was tested and compared to the ones of the Chelex- and Metsorb-DGT (Figure 1, panels B and C). This work showed that the DGT measurements were not dependent on the ionic strength value (up to 700 mmol L^{-1} adjusted with $NaNO_3$). The Monophos-DGT uptake of inorganic U(VI) species was not impacted by the competitive binding of Ca^{2+} and Mg^{2+}, whereas it was clearly a limitation for the Chelex-DGT samplers. The Monophos-DGT response was not impacted by the presence of HCO_3^- up to 5 mmol L^{-1}; while the application of the Metsorb-DGT sampler was possible only in continental waters with a HCO_3^- not higher than 1.5 mmol L^{-1}. Only the Monophos-DGT sampler led to reliable DGT measurements in synthetic seawater up to 96 h, confirming its robustness.

In situ deployments in two French rivers (Œuf and Essonne) yielded accurate $c_{T,U}$ by Monophos-DGT samplers, whereas measurements with Chelex- and Metsorb-DGT samplers suffered interferences due to the elevated concentration levels of alkali-earth metals and bicarbonate, respectively.

This work has highlighted some limitations in the complete understanding of DGT measurement in moderately basic waters. Indeed, without a minimum of speciation data (obtained, *e.g.*, by hyphenated physico-chemical analyses with thermodynamic calculations) and individual diffusion coefficient values for U(VI) complexes [52], it is not possible to accurately compute $\bar{D}^{mdl}$. The alternative used in this work is to measure $\bar{D}^{mdl}$ on the site by means of DGT samplers equipped with various diffusive gel thicknesses, leading to accurate average $c_{T,U}$ determinations during deployment time of 24-72 h (lower deployment time are recommended if the concentration level is sufficient). As a linear plot of the reciprocal M_{DGT} versus δ^{mdl} was observed ($R^2 \geq 0.95$), the slope could be used to calculate $\bar{D}^{mdl}$ (as in sections 4.2.1). In addition to the retrieved parameters, this methodology offers the advantage of qualifying the nature of U(VI) DGT-labile complexes in the deployment solution (*e.g.*, the found $\bar{D}^{mdl}$ will reflect the dissolved speciation). If dedicated *in situ* studies are not feasible, one practical approach for waters like those analyzed here, is to adopt our found $\bar{D}^{mdl} = 4.63 \times 10^{-10}$ m^2 s^{-1}.

The use of double resin configuration is very scarce in the literature [68], and its full interpretation requires further experimentation and modelling, to understand well how the medium impacts on the accumulation (influence of non-studied interferences, influence of dissolved organic matter, formation of precipitates inside of DGT samplers, temperature changes, etc.). To obtain them, future DGT research requires more commercially-available caps with different thicknesses to progress in the understanding of DGT devices, notably when the binding agent does not act as a perfect sink. Furthermore, we combined DGT sampling with elemental and isotopic measurements for water source tracing. These simultaneous measurements were successfully performed during field applications, opening new perspectives for environmental applications [11] such as highlighting anthropogenic activities in the environment around uranium processing plants [69-71], nuclear facilities [72-75] or mining areas [76] by using U minor isotopes (^{234}U, ^{235}U and ^{236}U) that require preconcentration before quantification.

Acknowledgements

This work has been supported by the ANR (French National Research Agency), under the "Investissement d'Avenir" framework program [Number ANR-17-CE08-0053]. The authors thank Graver Technologies (www.gravertech.com) for the provision of the Metsorb® HMRP 50 products used in this study. All experiments were performed at LUTECE (the SEDRE's experimental platform), and isotopic measurements at PATERSON (the IRSN's mass spectrometry platform). This is PATERSON contribution n°16. This work benefited from the knowledge acquired on the spatial and temporal distribution of U concentration in the Œuf-Essonne River through the research project UTOPIA conducted by Dr Mathilde Zebracki (IRSN) and a financial support for the field campaign through the research project NEPTUNE conducted by Dr Josselin Gorny (IRSN), all being funded by the French program NEEDS. Cyrielle Jardin, Gilles Alcalde, Olivier Diez and Patrice Blaise (IRSN) are gratefully thanked for their technical support, Dr. Laurent Guimier and Matthieu Pages (this is IRSN LAB contribution n°1) for the three-dimensional printing of HIPS rings, Jean Schoch, Dr. Pierre-Jean Superville and Pr Gabriel Billon (LASIRE) for their contribution in the second field campaign, and Charlotte Cazala (IRSN) for her help in administration project. Dr. Clémence Houzé and all the staff from the syndicate in charge of the supervision of the Essonne River (SIARCE) are gratefully thanked for allowing us to access a protected site during the second field campaign. Support from the Spanish Ministry of Science and Innovation is gratefully acknowledged (MCIN/AEI/ 10.13039/501100011033, projects PID2019-107033GB-C21 and PID2022-140312NB-C21).

Credit author statements

Josselin Gorny: Conceptualization, Methodology, DGT experiments, Physico-chemical measurements (Alkalinity, ICP-OES and ICP-MS), Thermodynamic calculations; Validation, Investigation, Resources, Writing – original draft, Writing – review & editing; Project administration; Supervision; **Charlotte Lafont:** DGT experiments, Physico-chemical measurements (Alkalinity, IC, ICP-OES and ICP-MS), Validation; **Clémentine Sapey:** DGT experiments, Physico-chemical measurements (ICP-MS); **Steffen Happel:** Conceptualization, Methodology, Ressources; **Alkiviadis Gourgiotis:** Methodology for isotopic measurement, Ressources; **Laureline Février:** Thermodynamic calculations, writing – review & editing; **Josep Galceran:** Conceptualization, Methodology, Development of new analytical expressions, Writing – original draft, Writing – review & editing;

References

[1] T. Mathews, K. Beaugelin-Seiller, J. Garnier-Laplace, R. Gilbin, C. Adam, C. Della-Vedova, A Probabilistic Assessment of the Chemical and Radiological Risks of Chronic Exposure to Uranium in Freshwater Ecosystems, Environmental science & technology, 43 (2009) 6684-6690.
[2] M. Leermakers, V. Phrommavanh, J. Drozdzak, Y. Gao, J. Nos, M. Descostes, DGT as a useful monitoring tool for radionuclides and trace metals in environments impacted by uranium mining: Case study of the Sagnes wetland in France, Chemosphere, 155 (2016) 142-151.
[3] J. Drozdzak, M. Leermakers, Y. Gao, M. Elskens, V. Phrommavanh, M. Descostes, Uranium aqueous speciation in the vicinity of the former uranium mining sites using the diffusive gradients in thin films and ultrafiltration techniques, Analytica Chimica Acta, 913 (2016) 94-106.
[4] J.H. Pedrobom, C.E. Eismann, A.A. Menegário, J.A. Galhardi, K.S. Luko, T.d.A. Dourado, C.H. Kiang, In situ speciation of uranium in treated acid mine drainage using the diffusion gradients in thin films technique (DGT), Chemosphere, 169 (2017) 249-256.
[5] A. Husson, M. Leermakers, M. Descostes, V. Lagneau, Environmental geochemistry and bioaccumulation/bioavailability of uranium in a post-mining context – The Bois-Noirs Limouzat mine (France), Chemosphere, 236 (2019) 124341.
[6] A. Husson, Impact de la composition minéralogique des sédiments sur la biodisponibilité de l'Uranium: Une approche intégrant laboratoire-terrain-bioindicateur-calcul de spéciation, Doctoral dissertation, Paris Sciences et Lettres (ComUE), 2019.
[7] A. Martin, G. Montavon, C. Landesman, A combined DGT - DET approach for an in situ investigation of uranium resupply from large soil profiles in a wetland impacted by former mining activities, Chemosphere, 279 (2021) 130526.
[8] J.A. Galhardi, J.W.V. de Mello, K.J. Wilkinson, Bioaccumulation of potentially toxic elements from the soils surrounding a legacy uranium mine in Brazil, Chemosphere, 261 (2020) 127679.
[9] H. Gemeiner, A.A. Menegário, P.N. Williams, A.E. Matavelli Rosa, C.A. Santos, J.H. Pedrobom, L.P. Elias, H.K. Chang, Lability and bioavailability of Co, Fe, Pb, U and Zn in a uranium mining restoration site using DGT and phytoscreening, Environmental Science and Pollution Research, 28 (2021) 57149-57165.
[10] G.S.C. Turner, G.A. Mills, M.J. Bowes, J.L. Burnett, S. Amos, G.R. Fones, Evaluation of DGT as a long-term water quality monitoring tool in natural waters; uranium as a case study, Environmental Science: Processes & Impacts, 16 (2014) 393-403.
[11] L. Pantoja, H. Garelick, A critical review of the quantification, analysis and detection of radionuclides in the environment using diffusive gradients in thin films (DGT): advances and perspectives, Pure and Applied Chemistry, (2023).
[12] V. Smolíková, P. Pelcová, A. Ridošková, M. Leermakers, Diffusive Gradients in Thin-films technique for uranium monitoring along a salinity gradient: A comparative study on the performance of Chelex-100, Dow-PIWBA, Diphonix, and Lewatit FO 36 resin gels in the Scheldt estuary, Talanta, 240 (2022) 123168.
[13] J. Drozdzak, M. Leermakers, Y. Gao, V. Phrommavanh, M. Descostes, Evaluation and application of Diffusive Gradients in Thin Films (DGT) technique using Chelex®-100, Metsorb™ and Diphonix® binding phases in uranium mining environments, Analytica Chimica Acta, 889 (2015) 71-81.
[14] G.S.C. Turner, G.A. Mills, J.L. Burnett, S. Amos, G.R. Fones, Evaluation of diffusive gradients in thin-films using a Diphonix® resin for monitoring dissolved uranium in natural waters, Analytica Chimica Acta, 854 (2015) 78-85.

[15] C.M. Hutchins, J.G. Panther, P.R. Teasdale, F. Wang, R.R. Stewart, W.W. Bennett, H. Zhao, Evaluation of a titanium dioxide-based DGT technique for measuring inorganic uranium species in fresh and marine waters, Talanta, 97 (2012) 550-556.
[16] J. Drozdzak, M. Leermakers, Y. Gao, V. Phrommavanh, M. Descostes, Novel speciation method based on Diffusive Gradients in Thin Films for in situ measurement of uranium in the vicinity of the former uranium mining sites, Environmental Pollution, 214 (2016) 114-123.
[17] J.E. Lartigue, B. Charrasse, B. Reile, M. Descostes, Aqueous inorganic uranium speciation in European stream waters from the FOREGS dataset using geochemical modelling and determination of a U bioavailability baseline, Chemosphere, 251 (2020) 126302.
[18] V. Moulin, J. Tits, G. Ouzounian, Actinide Speciation in the Presence of Humic Substances in Natural Water Conditions, Radiochimica Acta, 58-59 (1992) 179-190.
[19] A. Křepelová, S. Sachs, G. Bernhard, Uranium(VI) sorption onto kaolinite in the presence and absence of humic acid, Radiochimica Acta, 94 (2006) 825-833.
[20] G.S. Turner, G.A. Mills, P.R. Teasdale, J.L. Burnett, S. Amos, G.R. Fones, Evaluation of DGT techniques for measuring inorganic uranium species in natural waters: interferences, deployment time and speciation, Analytica Chimica Acta, 739 (2012) 37-46.
[21] Y. Wang, S. Ding, M. Gong, S. Xu, W. Xu, C. Zhang, Diffusion characteristics of agarose hydrogel used in diffusive gradients in thin films for measurements of cations and anions, Analytica Chimica Acta, 945 (2016) 47-56.
[22] H. Zhang, W. Davison, Performance Characteristics of Diffusion Gradients in Thin Films for the in Situ Measurement of Trace Metals in Aqueous Solution, Analytical chemistry, 67 (1995) 3391-3400.
[23] W.W. Bennett, P.R. Teasdale, J.G. Panther, D.T. Welsh, D.F. Jolley, New diffusive gradients in a thin film technique for measuring inorganic arsenic and selenium (IV) using a titanium dioxide based adsorbent, Analytical chemistry, 82 (2010) 7401-7407.
[24] IRSN PATERSON - Plateforme de spectrométrie de masse dédiée aux activité de recherche en radioprotection et sûreté nucléaire https://doi.org/10.57876/8HJP-4744.
[25] J. Hiess, D.J. Condon, N. McLean, S.R. Noble, $^{238}U/^{235}U$ Systematics in Terrestrial Uranium-Bearing Minerals, Science, 335 (2012) 1610-1614.
[26] W.A. Russell, D.A. Papanastassiou, T.A. Tombrello, Ca isotope fractionation on the Earth and other solar system materials, Geochimica et Cosmochimica Acta, 42 (1978) 1075-1090.
[27] H. Cheng, R.L. Edwards, J. Hoff, C.D. Gallup, D.A. Richards, Y. Asmerom, The half-lives of uranium-234 and thorium-230, Chemical Geology, 169 (2000) 17-33.
[28] K.W. Warnken, H. Zhang, W. Davison, Accuracy of the Diffusive Gradients in Thin-Films Technique: Diffusive Boundary Layer and Effective Sampling Area Considerations, Analytical chemistry, 78 (2006) 3780-3787.
[29] H. Cheng, Y. Li, H. Pouran, W. Davison, H. Zhang, Investigation of diffusion and binding properties of uranium in the diffusive gradients in thin-films technique, Environmental Chemistry, 19 (2022) 263-273.
[30] J.L. Levy, H. Zhang, W. Davison, J. Puy, J. Galceran, Assessment of trace metal binding kinetics in the resin phase of diffusive gradients in thin films, Analytica Chimica Acta, 717 (2012) 143-150.
[31] J. Gorny, C. Jardin, O. Diez, J. Galceran, A. Gourgiotis, S. Happel, F. Coppin, L. Février, C. Simonucci, C. Cazala, Dissolved iodide in marine waters determined with Diffusive Gradients in Thin-films technique, Analytica Chimica Acta, 1177 (2021) 338790.

[32] K. Grasshoff, K. Kremling, M. Ehrhardt, Methods of seawater analysis, WILEY-VCH Verlag GmbH, D-69469 Weinheim (Federal Republic of Germany), 1999 1999.
[33] M. Zebracki, C. Marlin, T. Gaillard, J. Gorny, O. Diez, V. Durand, C. Lafont, C. Jardin, V. Monange, Elevated uranium concentration and low activity ratio (234U/238U) in the Œuf river as the result of groundwater–surface water interaction (Essonne river valley, South of Paris Basin, France), Science of The Total Environment, 876 (2023) 162537.
[34] D.L. Parkhurst, C. Appelo, Description of input and examples for PHREEQC version 3: a computer program for speciation, batch-reaction, one-dimensional transport, and inverse geochemical calculations, US Geological Survey, 2013.
[35] P.E. Reiller, M. Descostes, Development and application of the thermodynamic database PRODATA dedicated to the monitoring of mining activities from exploration to remediation, Chemosphere, 251 (2020) 126301.
[36] P.E. Reiller, The PRODATA Thermochemical database. A database applied for uranium mining operations, Commissariat à l'énergie atomique et aux énergies alternatives, Report CEA-R-6573, 2022.
[37] J.L. Levy, H. Zhang, W. Davison, J. Puy, J. Galceran, Assessment of trace metal binding kinetics in the resin phase of diffusive gradients in thin films, Analytica Chimica Acta, 717 (2012) 143-150.
[38] J. Puy, J. Galceran, C. Rey-Castro, Interpreting the DGT Measurement: Speciation and Dynamics, in: W. Davison (Ed.) Diffusive Gradients in Thin-Films for Environmental Measurements, Cambridge University Press, Cambridge, 2016, pp. 93-122.
[39] J. Gorny, L. Lesven, G. Billon, D. Dumoulin, C. Noiriel, C. Pirovano, B. Madé, Determination of total arsenic using a novel Zn-ferrite binding gel for DGT techniques: Application to the redox speciation of arsenic in river sediments, Talanta, 144 (2015) 890-898.
[40] J. Gorny, D. Dumoulin, V. Alaimo, L. Lesven, C. Noiriel, B. Madé, G. Billon, Passive sampler measurements of inorganic arsenic species in environmental waters: A comparison between 3-mercapto-silica, ferrihydrite, Metsorb®, zinc ferrite, and zirconium dioxide binding gels, Talanta, 198 (2019) 518-526.
[41] J. Gorny, A. Gourgiotis, F. Coppin, L. Février, H. Zhang, C. Simonucci, Better understanding and applications of ammonium 12-molybdophosphate-based diffusive gradient in thin film techniques for measuring Cs in waters, Environmental Science and Pollution Research, 26 (2019) 1994-2006.
[42] G.S.C. Turner, G.A. Mills, P.R. Teasdale, J.L. Burnett, S. Amos, G.R. Fones, Evaluation of DGT techniques for measuring inorganic uranium species in natural waters: Interferences, deployment time and speciation, Analytica Chimica Acta, 739 (2012) 37-46.
[43] M. Gregusova, B. Docekal, New resin gel for uranium determination by diffusive gradient in thin films technique, Analytica Chimica Acta, 684 (2011) 142-146.
[44] Ø.A. Garmo, O. Røyset, E. Steinnes, T.P. Flaten, Performance Study of Diffusive Gradients in Thin Films for 55 Elements, Analytical chemistry, 75 (2003) 3573-3580.
[45] D. Devillers, R. Buzier, A. Charriau, G. Guibaud, Improving elution strategies for Chelex®-DGT passive samplers, Analytical and Bioanalytical Chemistry, 409 (2017) 7183-7189.
[46] A. Kreuzeder, J. Santner, H. Zhang, T. Prohaska, W.W. Wenzel, Uncertainty Evaluation of the Diffusive Gradients in Thin Films Technique, Environmental science & technology, 49 (2015) 1594-1602.
[47] R. Rich, Titanium through Rutherfordium, Inorganic Reactions in Water, Springer Berlin Heidelberg, Berlin, Heidelberg, 2007, pp. 91-100.

[48] A.A. Ammann, Arsenic speciation by gradient anion exchange narrow bore ion chromatography and high resolution inductively coupled plasma mass spectrometry detection, Journal of Chromatography A, 1217 (2010) 2111-2116.
[49] S. Saverwyns, X. Zhang, F. Vanhaecke, R. Cornelis, L.U.C. Moens, R. Dams, Speciation of Six Arsenic Compounds Using High-performance Liquid Chromatography-Inductively Coupled Plasma Mass Spectrometry With Sample Introduction by Thermospray Nebulization, Journal of Analytical Atomic Spectrometry, 12 (1997) 1047-1052.
[50] D. Heitkemper, J. Creed, J. Caruso, F.L. Fricke, Speciation of arsenic in urine using high-performance liquid chromatography with inductively coupled plasma mass spectrometric detection, Journal of Analytical Atomic Spectrometry, 4 (1989) 279-284.
[51] R. Dahlqvist, H. Zhang, J. Ingri, W. Davison, Performance of the diffusive gradients in thin films technique for measuring Ca and Mg in freshwater, Analytica Chimica Acta, 460 (2002) 247-256.
[52] S. Kerisit, C. Liu, Molecular simulation of the diffusion of uranyl carbonate species in aqueous solution, Geochimica et Cosmochimica Acta, 74 (2010) 4937-4952.
[53] A.-L. Pommier, R. Buzier, S. Simon, G. Guibaud, Impact of low ionic strength on DGT sampling with standard APA gels: Effect of pH and analyte, Talanta, 222 (2021) 121413.
[54] L.P. Yezek, H.P. van Leeuwen, Donnan Effects in the Steady-State Diffusion of Metal Ions through Charged Thin Films, Langmuir, 21 (2005) 10342-10347.
[55] N. Fatin-Rouge, A. Milon, J. Buffle, R.R. Goulet, A. Tessier, Diffusion and Partitioning of Solutes in Agarose Hydrogels: The Relative Influence of Electrostatic and Specific Interactions, The Journal of Physical Chemistry B, 107 (2003) 12126-12137.
[56] V. Smolíková, P. Pelcová, A. Ridošková, M. Leermakers, Simultaneous determination of arsenic and uranium by the diffusive gradients in thin films technique using Lewatit FO 36: Optimization of elution protocol, Talanta, 228 (2021) 122234.
[57] G.S.C. Turner, The Application of the Passive Sampling Technique Diffusive Gradients in Thin-films (DGT) to the Measurement of Uranium in Natural Waters, Doctoral dissertation, University of Portsmouth, 2013.
[58] J. Gimpel, H. Zhang, W. Hutchinson, W. Davison, Effect of solution composition, flow and deployment time on the measurement of trace metals by the diffusive gradient in thin films technique, Analytica Chimica Acta, 448 (2001) 93-103.
[59] M. Jiménez-Piedrahita, A. Altier, J. Cecilia, J. Puy, J. Galceran, C. Rey-Castro, H. Zhang, W. Davison, Extending the Use of Diffusive Gradients in Thin Films (DGT) to Solutions Where Competition, Saturation, and Kinetic Effects Are Not Negligible, Analytical chemistry, 89 (2017) 6567-6574.
[60] D.R. Lide, CRC handbook of chemistry and physics, CRC press Boca Raton, FL, USA 2004.
[61] A. Altier, M. Jiménez-Piedrahita, C. Rey-Castro, J. Cecilia, J. Galceran, J. Puy, Accumulation of Mg to Diffusive Gradients in Thin Films (DGT) Devices: Kinetic and Thermodynamic Effects of the Ionic Strength, Analytical chemistry, 88 (2016) 10245-10251.
[62] S. Tankéré-Muller, W. Davison, H. Zhang, Effect of competitive cation binding on the measurement of Mn in marine waters and sediments by diffusive gradients in thin films, Analytica Chimica Acta, 716 (2012) 138-144.
[63] A. Stockdale, N.D. Bryan, Application of DGT to high pH environments: uptake efficiency of radionuclides of different oxidation states onto Chelex binding gel, Environmental Science: Processes & Impacts, 15 (2013) 1087-1091.

[64] R. Chiarizia, E.P. Horwitz, R.C. Gatrone, S.D. Alexandratos, A.Q. Trochimczuk, D.W. Crick, Uptake of metal ions by a new chelating ion-exchange resin. part 2: acid dependencies of transition and post-transition metal ions, Solvent Extraction and Ion Exchange, 11 (1993) 967-985.
[65] N. Suhr, M. Widdowson, F. McDermott, B.S. Kamber, Th/U and U series systematics of saprolite: importance for the oceanic 234U excess, Geochemical Perspectives Letters, 6 (2018) 17-22.
[66] J. Osmond, J. Cowart, The theory and uses of natural uranium isotopic variations in hydrology, Atomic Energy Review, 14 (1976) 621-679.
[67] E.D. Young, A. Galy, H. Nagahara, Kinetic and equilibrium mass-dependent isotope fractionation laws in nature and their geochemical and cosmochemical significance, Geochimica et Cosmochimica Acta, 66 (2002) 1095-1104.
[68] J. Sans-Duñó, J. Cecilia, J. Galceran, J. Puy, W. Baeyens, Y. Gao, Back Accumulation of Diffusive Gradients in Thin-Films Devices with a Stack of Resin Discs To Assess Availability of Metal Cations to Biota in Natural Waters, Environmental science & technology, 57 (2023) 7840-7848.
[69] M. Lin, J. Qiao, X. Hou, O. Dellwig, P. Steier, K. Hain, R. Golser, L. Zhu, 70-Year Anthropogenic Uranium Imprints of Nuclear Activities in Baltic Sea Sediments, Environmental science & technology, 55 (2021) 8918-8927.
[70] L. Pourcelot, B. Boulet, C. Le Corre, J. Loyen, C. Fayolle, D. Tournieux, W. Van Hecke, B. Martinez, J. Petit, Isotopic evidence of natural uranium and spent fuel uranium releases into the environment, Journal of Environmental Monitoring, 13 (2011) 355-361.
[71] L. Pourcelot, B. Boulet, C. Cossonnet, Contribution des isotopes de l'uranium à l'expertise des sources de ce radioélément dans l'environnement, Radioprotection, 46 (2011) 345-358.
[72] A. Morereau, H. Jaegler, K. Hain, P. Steier, R. Golser, A. Beaumais, H. Lepage, F. Eyrolle, C. Grosbois, C. Cazala, Deciphering sources of U contamination using isotope ratio signatures in the Loire River sediments: Exploring the relevance of 233U/236U and stable Pb isotope ratios, Chemosphere, 307 (2022) 135658.
[73] H. Jaegler, F. Pointurier, S. Diez-Fernández, A. Gourgiotis, H. Isnard, S. Hayashi, H. Tsuji, Y. Onda, A. Hubert, J.P. Laceby, O. Evrard, Reconstruction of uranium and plutonium isotopic signatures in sediment accumulated in the Mano Dam reservoir, Japan, before and after the Fukushima nuclear accident, Chemosphere, 225 (2019) 849-858.
[74] H. Jaegler, A. Gourgiotis, P. Steier, R. Golser, O. Diez, C. Cazala, Pushing Limits of ICP–MS/MS for the Determination of Ultralow 236U/238U Isotope Ratios, Analytical chemistry, 92 (2020) 7869-7876.
[75] H. Jaegler, A. Gourgiotis, A new milestone for ultra-low 236 U/238 U isotope ratio measurements by ICP-MS/MS, Journal of Analytical Atomic Spectrometry, 38 (2023) 1914-1919.
[76] A. Beaumais, A. Mangeret, D. Suhard, P. Blanchart, M. Neji, C. Cazala, A. Gourgiotis, Combined U-Pb isotopic signatures of U mill tailings from France and Gabon: A new potential tracer to assess their fingerprint on the environment, Journal of Hazardous Materials, 430 (2022) 128484.
[77] W. Li, J. Zhao, C. Li, S. Kiser, R. Jack Cornett, Speciation measurements of uranium in alkaline waters using diffusive gradients in thin films technique, Analytica Chimica Acta, 575 (2006) 274-280.
[78] W. Li, C. Li, J. Zhao, R.J. Cornett, Diffusive gradients in thin films technique for uranium measurements in river water, Analytica Chimica Acta, 592 (2007) 106-113.

[79] V. Phrommavanh, M. Leermakers, H. de Boissezon, J. Nos, M.-B. Koko, M. Descostes, Characterizing the Transport of Natural Uranium and its Decay Product 226Ra, Downstream from Former Mines in France, Procedia Earth and Planetary Science, 7 (2013) 693-696.
[80] A. Martin, C. Landesman, A. Lépinay, C. Roux, J. Champion, P. Chardon, G. Montavon, Flow period influence on uranium and trace elements release in water from the waste rock pile of the former La Commanderie uranium mine (France), Journal of Environmental Radioactivity, 208-209 (2019) 106010.
[81] J. Zhao, R.J. Cornett, C.L. Chakrabarti, Assessing the uranium DGT-available fraction in model solutions, Journal of Hazardous Materials, 384 (2020) 121134.
[82] H. Vandenhove, K. Antunes, J. Wannijn, L. Duquène, M. Van Hees, Method of diffusive gradients in thin films (DGT) compared with other soil testing methods to predict uranium phytoavailability, Science of The Total Environment, 373 (2007) 542-555.
[83] L. Duquène, H. Vandenhove, F. Tack, M. Van Hees, J. Wannijn, Diffusive gradient in thin films (DGT) compared with soil solution and labile uranium fraction for predicting uranium bioavailability to ryegrass, Journal of Environmental Radioactivity, 101 (2010) 140-147.
[84] J. Mihalík, P. Henner, S. Frelon, V. Camilleri, L. Février, Citrate assisted phytoextraction of uranium by sunflowers: Study of fluxes in soils and plants and resulting intra-planta distribution of Fe and U, Environmental and Experimental Botany, 77 (2012) 249-258.
[85] J.D. Chaplin, P.E. Warwick, A.B. Cundy, F. Bochud, P. Froidevaux, Novel DGT Configurations for the Assessment of Bioavailable Plutonium, Americium, and Uranium in Marine and Freshwater Environments, Analytical chemistry, 93 (2021) 11937-11945.
[86] J. Zhao, A study of uranium speciation in surface freshwaters using diffusive gradients in thin films, Doctoral dissertation, Carleton University, 2009.
[87] H. Österlund, Further characterisation and applications of the diffusive gradients in thin films technique: In situ measurements of anions and cations in environmental waters, Doctoral dissertation, Luleå tekniska universitet, 2011.
[88] G. Bucher, Développements analytiques pour la spéciation de l'uranium dans les branchies du poisson zèbre (Danio rerio) après exposition, Doctoral dissertation, Université de Pau, 2013.
[89] V. Smolíková, Determination of Trace Elements in the Aquatic Environment Using Diffusive Gradients in Thin Films Technique, Doctoral dissertation, Mendel University in Brno & Vrije Universiteit Brussel, 2021.
[90] A. Stockdale, W. Davison, H. Zhang, 2D simultaneous measurement of the oxyanions of P, V, As, Mo, Sb, W and U, Journal of Environmental Monitoring, 12 (2010) 981-984.
[91] M. Gregusova, B. Docekal, High resolution characterization of uranium in sediments by DGT and DET techniques ACA-S-12-2197, Analytica Chimica Acta, 763 (2013) 50-56.
[92] P. Byrne, C.C. Fuller, D.L. Naftz, R.L. Runkel, N.J. Lehto, W.L. Dam, Transport and speciation of uranium in groundwater-surface water systems impacted by legacy milling operations, Science of The Total Environment, 761 (2021) 143314.
[93] A. Chapman, Assessing the bioavailability of the radionuclides technetium-99, selenium-79 and uranium-238 in contaminated soils using the diffusive gradients in thin-films (DGT) technique, Lancaster University (United Kingdom) 2018.
[94] C. Vogel, M.C. Hoffmann, M.C. Taube, O. Krüger, R. Baran, C. Adam, Uranium and thorium species in phosphate rock and sewage sludge ash based phosphorus fertilizers, Journal of Hazardous Materials, 382 (2020) 121100.

Tables

Table 1: Literature survey on binding phases employed in DGT samplers to measure total or DGT-labile U concentrations in various media using the search engine Google Scholar with the following keywords: “Diffusive Gradient in Thin-films”, “binding phase”, “resin” and “Uranium”.

Binding phase(s)	Year of first application	Cumulative number of applications				Reference(s)
		Waters	Sediments	Soils	Wetland	
Chelex®-100 resin	2003	19	3	5	2	[2-9, 12, 13, 15, 16, 20, 29, 43, 44, 57, 63, 77-89]
Whatman® DE81	2006	4	/	/	/	[4, 77, 78, 86]
Dowex® 2×8	2007	1	/	/	/	[12]
Whatman® PE81	2009	2	/	/	/	[4, 86]
Polymer A	2009	1	/	/	/	[86]
Ferrihydrite	2010	1	1	/	/	[29, 90]
Spheron-Oxin® 1000	2011	1	1	/	/	[43, 91]
Metsorb™ HMRP 50	2012	7	/	/	/	[10, 13, 15, 16, 20, 29, 57, 92]
MnO_2	2012	1	/	/	/	[20, 57]
Diphonix®	2015	4	/	/	/	[12-14, 16, 57]
Dow-PIWBA	2016	2	1	/	/	[3, 5, 6, 12, 16, 89]
Chelex-100® + ferrihydrite	2018	1	/	1	/	[93]
Chelex-100® + Metsorb™ HMRP 50	2020	/	/	1	/	[94]
Lewatit® FO 36	2021	3	/	/	/	[12, 56, 89]
KMS-1	2021	1	/	/	/	[85]
Monophos®	2022	1	/	/	/	This study

Table 2: Physico-chemical characteristics of deployment solutions (*i.e.*, of Volvic® and Vittel® waters after equilibration with the atmosphere and of the surface waters of the Œuf and Essonne river) followed by U(VI) speciation predictions according to the speciation program PHREEQC version 3.6.2.15100 with the database PRODATA version 1.5.2. White precipitates in Vittel water were observed after equilibration with the atmosphere.

	Element/dissolved species	Volvic	Vittel	Seawater	Œuf River			Essonne River	Unit
					SP1	SP2	SP3	SP4	
Physico-chemical composition	Ca^{2+}	0.39±0.02	3.49±0.23	13.6	3.00±0.09	3.26±0.19	3.35±0.14	2.36±0.04	mmol L^{-1}
	Mg^{2+}	0.44±0.02	2.05±0.09	114	0.10±0.01	0.25±0.01	0.26±0.01	0.21±0.01	mmol L^{-1}
	Na^{+}	0.50±0.03	0.21±0.01	471	0.46±0.03	0.52±0.02	0.76±0.03	0.44±0.01	mmol L^{-1}
	K^{+}	0.14±0.01	0.05±0.01	9.46	0.07±0.01	0.61±0.05	0.27±0.04	0.13±0.02	mmol L^{-1}
	DOC	/	/	/	0.56±0.05	0.22±0.03	0.17±0.01	0.15±0.01	mmol L^{-1}
	HCO_3^{-}	1.19±0.06	1.03±0.05	2.38	4.00±0.40	4.95±0.87	4.55±0.73	4.88±0.06	mmol L^{-1}
	Cl^{-}	0.49±0.01	0.22±0.01	675	0.80±0.03	1.15±0.05	1.30±0.02	0.73±0.02	mmol L^{-1}
	SO_4^{2-}	0.08±0.01	4.28±0.16	28.2	0.36±0.01	0.31±0.01	0.28±0.01	0.20±0.01	mmol L^{-1}
	NO_3^{-}	0.12±0.01	/	/	0.65±0.04	0.45±0.01	0.59±0.01	0.46±0.01	mmol L^{-1}
	U	78.57±8.40	67.64±0.84	78.15±0.42	29.71±0.42	70.42±0.88	56.72±0.63	17.20±0.34	nmol L^{-1}
	pH	8.1±0.2	8.1±0.2	8.22±0.1	8.4±0.1	8.1±0.1	8.4±0.1	8.1±0.1	None
	Conductivity	220±10	900±10	/	636±5	774±10	759±7	572±10	µS cm^{-1}
	Salinity	/	/	34.8	/	/	/	/	None
U(VI) speciation predictions)	$Ca_2UO_2(CO_3)_3$ (aq)	59	66	11	75	75	75	67	%
	$CaUO_2(CO_3)_3^{2-}$	26	31	25	25	25	25	33	%
	$MgUO_2(CO_3)_3^{2-}$	12	3	48	0	0	0	0	%
	$UO_2(CO_3)_3^{4-}$	2	0.4	16	0	0	0	0	%
	$UO_2(CO_3)_2^{2-}$	1	0.1	0	0	0	0	0	%

Table 3: Effective diffusion coefficient (mean ± standard deviation) determined from DGT-time series experiments or using ADBL experiments in 10 mmol L^{-1} $NaNO_3$ at various pH values (3-9). Sodium bicarbonate addition was employed in our study, as in [13, 16, 56]. Data obtained in Volvic® waters and during field calibration in the surface waters of the Essonne are in bold to better discriminate them from experiments performed in the lab. The uncertainties of the diffusion coefficient values are given by the respective authors. List of superscripts used in the table: "?" nature of the filter not found; "a" cellulose nitrate filter membrane; "b" polyethersulfone filter membrane; "c" polyvinylidiene fluoride filter membrane; "A" agarose-polyacrylamide diffusive gel; "B" agarose diffusive gel; "C" restricted agarose-polyacrylamide diffusive gel "1" Chelex®-100 resin; "2" Spheron-Oxin® 1000 resin; "3" Metsorb™ HMRP 50 adsorbent; "4" Diphonix® resin; "5" Dow-PIWBA resin; "6" Lewatit® FO 36 adsorbent; "7" Ferrihydrite binding gel; "8" Monophos resin. "*" indicates that the D^{eff} values were recalculated at 25°C by us using Stokes-Einstein law.

pH	$\overline{D}^{mdl}$ (× 10^{-10} m^2 s^{-1} at 25°C)	δ^{dbl} (µm)	Reference(s)
4.7	4.80 ± 0.96^{aA1}	≈ 100	[44]
5.0	4.70 ± 0.61^{aA1}		
5.4	4.00 ± 0.44^{aA1}		
5.9	3.40 ± 0.65^{aA1}		
6.4	4.39 ± 0.01^{bA1}	Data not found	[43]
6.4	4.19 ± 0.10^{bB1}		
3.0	$2.62\pm0.13^{?A1*}$	Data not found	[15]
3.5	$3.15\pm0.13^{?A1*}$		
4.9	$4.56\pm0.26^{?A1*}$		
6.0	$3.64\pm0.11^{?A1*}$		
6.5	$3.64\pm0.26^{?A1*}$		
7.0	$3.05\pm0.26^{?A1*}$		
7.7	$4.71\pm0.53^{?A1*}$		
8.1	$4.35\pm0.21^{?A1*}$		
3.0	4.07 ± 0.09^{cA1}; 4.97 ± 0.24^{cA3}; 4.55 ± 0.26^{cA4}; 5.02 ± 0.41^{cA5}	Data not found	[13, 16]
4.0	4.42 ± 0.15^{cA1}; 4.65 ± 0.27^{cA3}; 4.66 ± 0.27^{cA4}; 5.37 ± 0.35^{cA5}		
5.0	3.89 ± 0.29^{cA1}; 4.13 ± 0.10^{cA3}; 3.90 ± 0.69^{cA4}; 4.63 ± 0.12^{cA5}		
6.0	4.25 ± 0.21^{cA1}; 4.81 ± 0.17^{cA3}; 4.56 ± 0.82^{cA4}; 4.05 ± 0.14^{cA5}		
7.0	4.34 ± 0.44^{cA1}; 5.03 ± 0.38^{cA3}; 3.84 ± 0.13^{cA4}; 4.95 ± 0.35^{cA5}		
8.0	4.63 ± 0.28^{cA1}; 4.82 ± 0.25^{cA3}; 4.19 ± 0.12^{cA4}; 5.13 ± 0.13^{cA5}		
9.0	4.13 ± 0.79^{cA1}; 4.35 ± 0.49^{cA3}; 4.22 ± 0.32^{cA4}; 5.15 ± 0.78^{cA5}		
7.6	4.38 ± 0.06^{bA6}	Data not found	[16]
3.2	4.86 ± 0.24^{bA1}	<170	[29]
4.3	4.45 ± 0.13^{bA1}		
5.4	5.01 ± 0.15^{bA1}		
6.2	4.67 ± 0.07^{bA1}		
7.2	4.58 ± 0.09^{bA1}; 4.51 ± 0.08^{bA1}; 5.26 ± 0.17^{bA3}; 3.30 ± 0.15^{bA7}		
5.5	$3.20\pm?^{bC1}$; $5.50\pm?^{bA1}$; $6.70\pm?^{bB1}$		
3	6.34 ± 0.47^{bB8} (10 mmol L^{-1} $NaNO_3$)	86	This study
8	6.24 ± 0.26^{bB8} (10 mmol L^{-1} $NaNO_3$ and 1 mmol L^{-1} HCO_3^-)		
8-8.4	**4.63 ± 0.10^{bB8} (Volvic® water)**		
8.1	**4.35 ± 0.31^{bB8} (Essonne River)**		

Figures

Figure 1: Overview of this work, with the main novelties highlighted in purple colour. Different experiment types are indicated by different background colours.

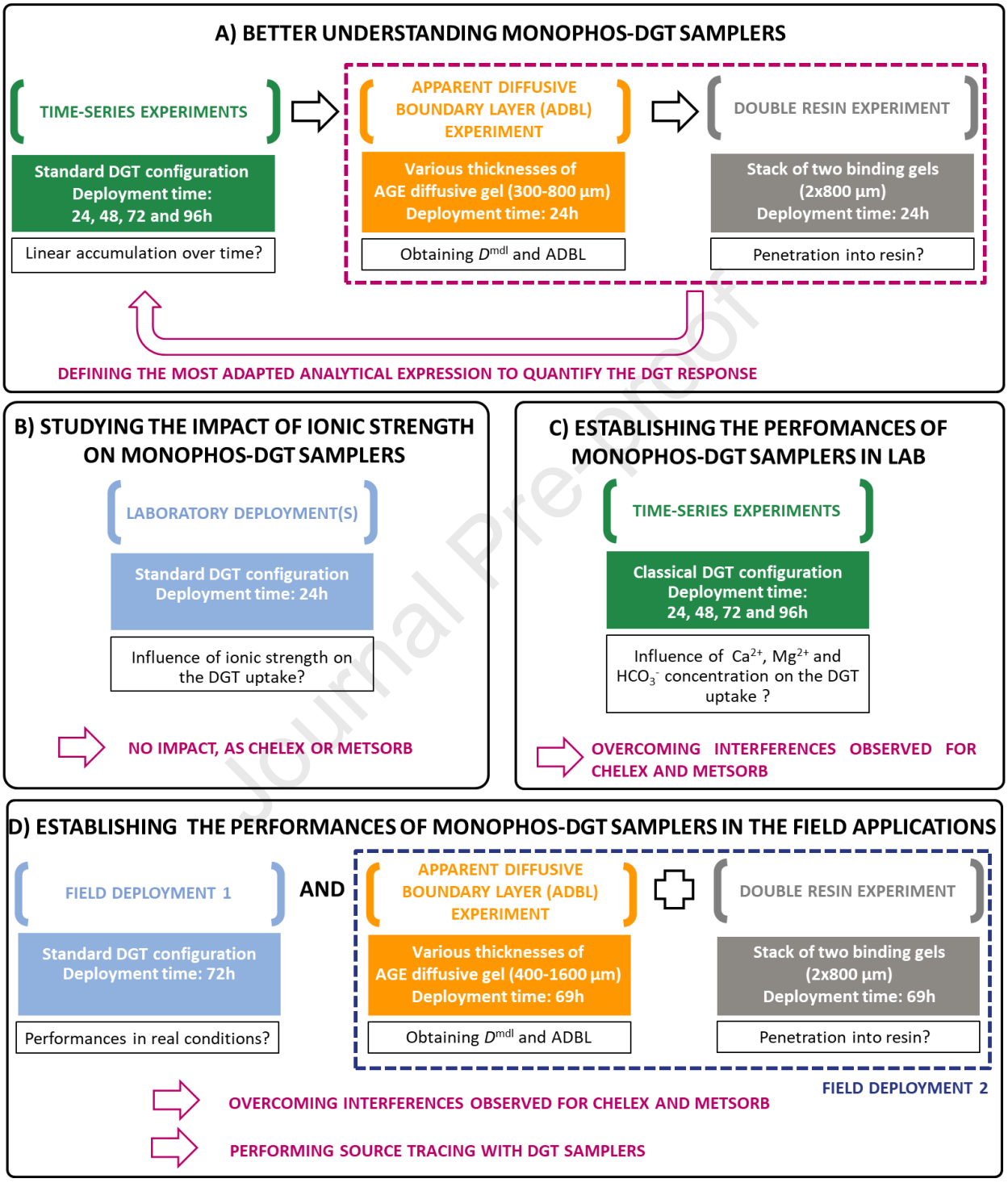

Figure 2: Elution factor (f_e) for U(VI) computed from the immersion of Chelex-, Metsorb- or Monophos-binding gels in HNO_3, HEDPA or HNO_3/H_2O_2 solution (all at 1 mol L^{-1}). Black dashed line corresponds to the minimum acceptable f_e for U(VI) (75%). Experimental conditions: polypropylene tube; 3 mL of eluent solution; 24 h of immersion.

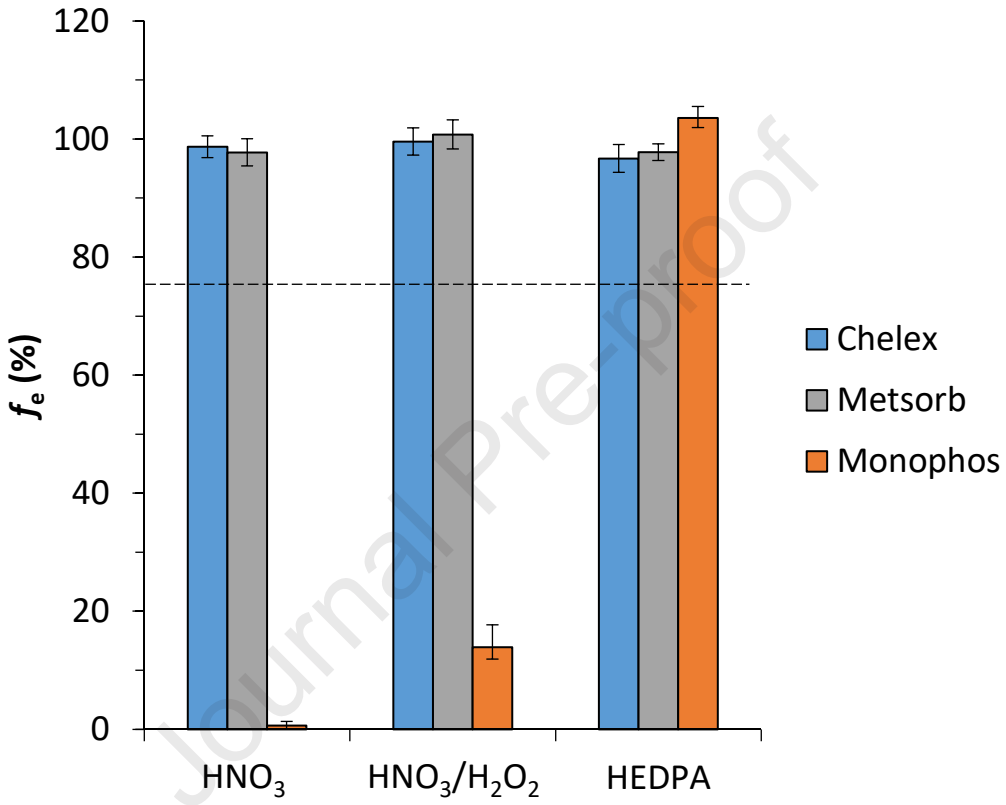

Figure 3: Evolution of the mass of U(VI) species accumulated by the Monophos-DGT sampler (orange color) as a function of time (bullets for experiments and grey dashed line for linear regression curve) with a fixed δ^{mdl} of 0.094 cm in panels A. In panels B, for a deployment time of 24 hours, the DBL thickness is found from the regression (dashed line) of the invers of the experimental accumulated masses (markers) in front of the thickness of material diffusion layers. One bullet shape is used for each kind of deployment conditions: + for [$NaNO_3$] = 10 mmol L^{-1} at pH 3; × for [$NaNO_3$] = 10 mmol L^{-1} at pH 8; □ for Volvic® waters. Black continuous line corresponds to the DGT response calculated using Eq (6) with a $\bar{D}^{mdl}$ value of 6.34±0.47, 6.24±0.26 and 4.63±0.10× 10^{-10} m^2s^{-1}at 25°C for the simple matrix at pH 3, the simple matrix at pH 8 and in Volvic® waters, respectively, $\bar{k}'_{a,R} = 2.24 \times 10^{-2}$ s^{-1} and $\delta^{dbl} = 86.11$ µm . Black dotted lines define ±15% acceptable error on the DGT measurement, and grey dashed line is the linear regression obtained from experimental points. Temperature and $c_{T,U}$ are reported in Tables S2 and S3.

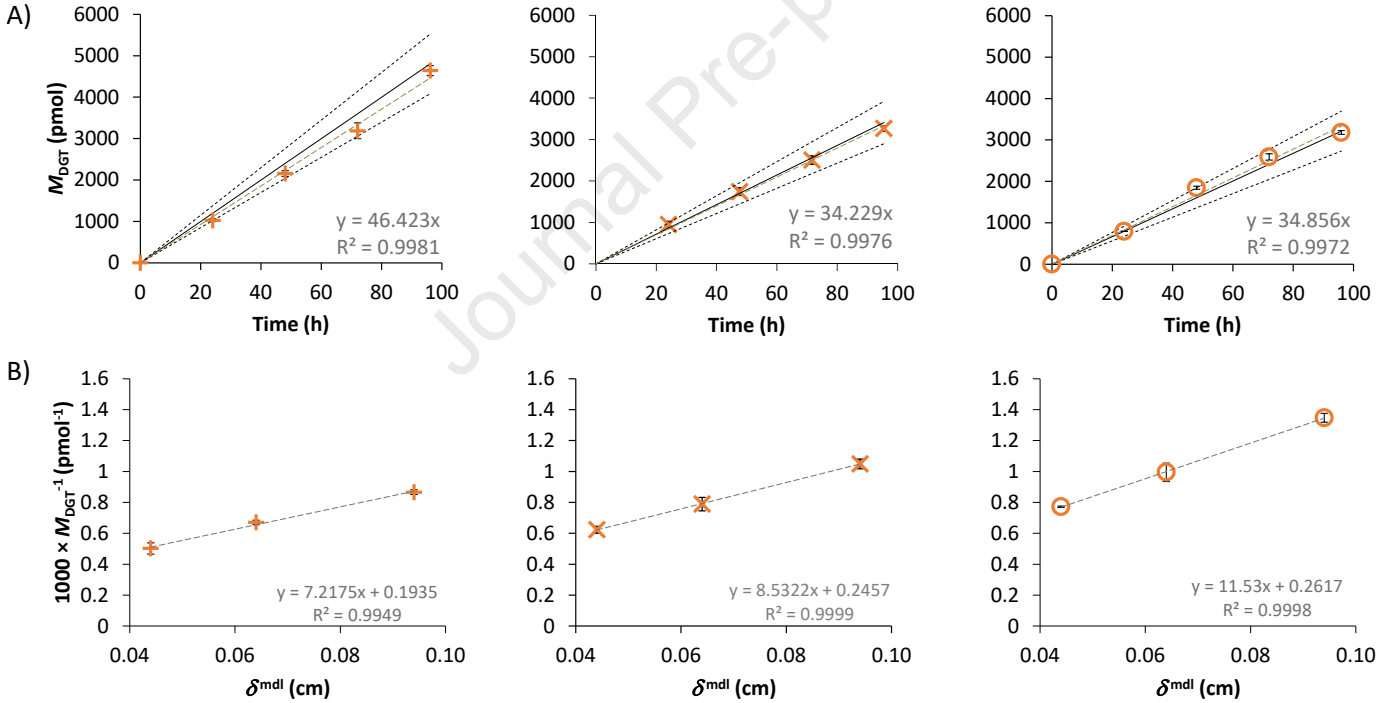

Figure 4: Effect of ionic strength on the DGT uptake of U(VI) species using Chelex-, Metsorb- and Monophos-binding gels (blue, grey and orange colour, respectively). Black horizontal dashed lines correspond to ±15% acceptable error on the DGT measurement. Experimental conditions: deployment time of 24 h; [$NaNO_3$] = 1-700 mmol L^{-1}; [$NaHCO_3$] = 1 mmol L^{-1}; $c_{T,U}$ = 71-84 nmol L^{-1}; T = 23.0-24.7°C.

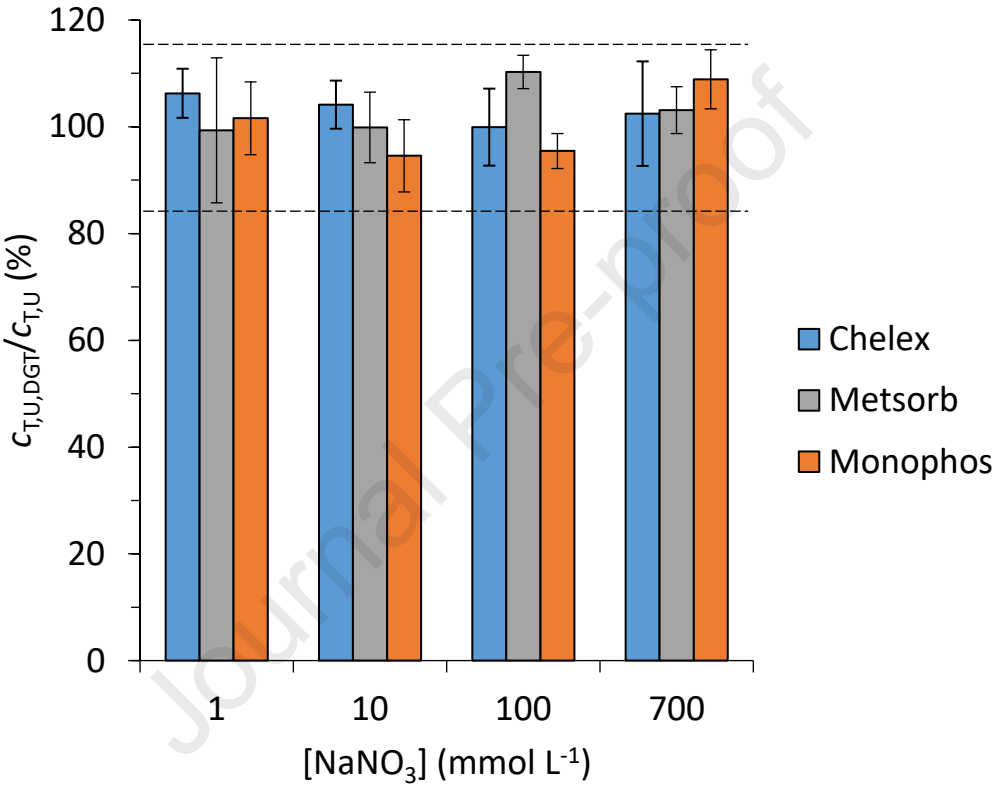

Figure 5: U accumulation over time with Chelex-, Metsorb- and Monophos-DGT samplers (experimental points in blue, grey and orange markers, respectively) in the complex matrices. A different marker shape is used for each kind of deployment solution: □ for Volvic® waters; ◊ for Vittel® waters; ⌴ for synthetic seawater. Experimental data are also available in Tables S3 and S4. Black continuous line corresponds to the DGT response calculated using Eq (6) with $\bar{D}^{mdl} = 4.63 \times 10^{-10}$ m^2 s^{-1} at 25°C , $\bar{k}'_{a,R} = 2.24 \times 10^{-2}$ s^{-1} at 25°C and $\delta^{dbl} = 86.11$ µm . Black dotted lines indicate ±15% acceptable error on the DGT measurement, and grey dashed line stands for the linear regression obtained from experimental points.

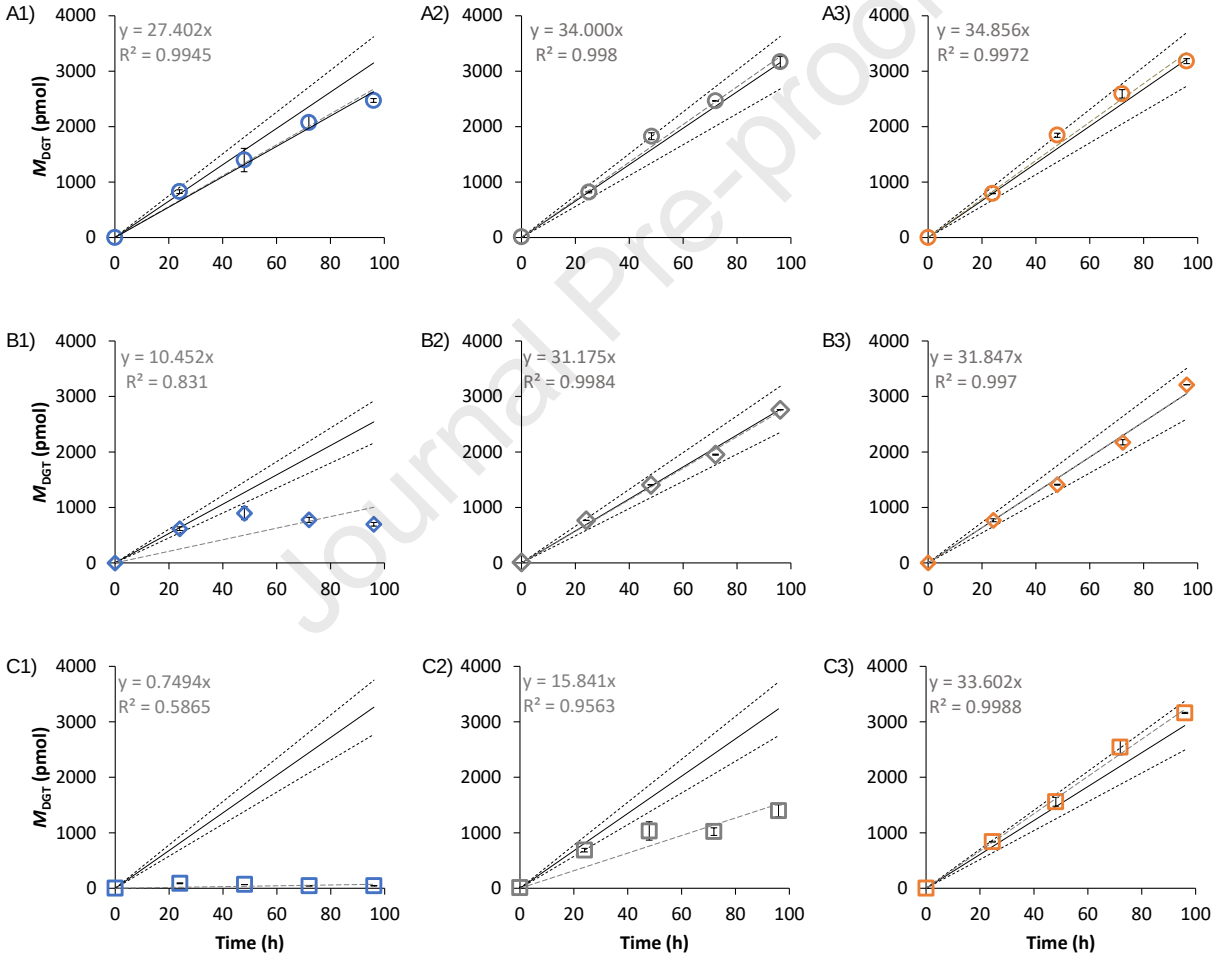

Figure 6: Illustration of deployment of DGT samplers in A) the Œuf and B) the Essonne rivers (Essonne, France). Results of DGT deployment in the two French rivers: C) $c_{T,U,DGT} / c_{T,U}$ values for the different binding materials and D) ($^{234}U/^{238}U$) activity ratios as a function of sampling point. The colour bar/bullet for Chelex-, Metsorb-, and Monophos-DGT samplers are blue, grey and orange, respectively. Intercomparison of DGT samplers in the Œuf River was performed in 2021 (SP1, SP2 and SP3), and the complementary campaign using only Monophos-DGT samplers in the Essonne River was made in 2023 (SP4). Parameters employed to calculate $c_{T,U,DGT}$ using Eq (11) were: $\bar{D}^{mdl} = 4.35 \times 10^{-10}$ m^2 s^{-1} at 25°C, and ADBL=181.40 µm. Lines for acceptable error in the DGT measurement as in Figures 3 and 4.

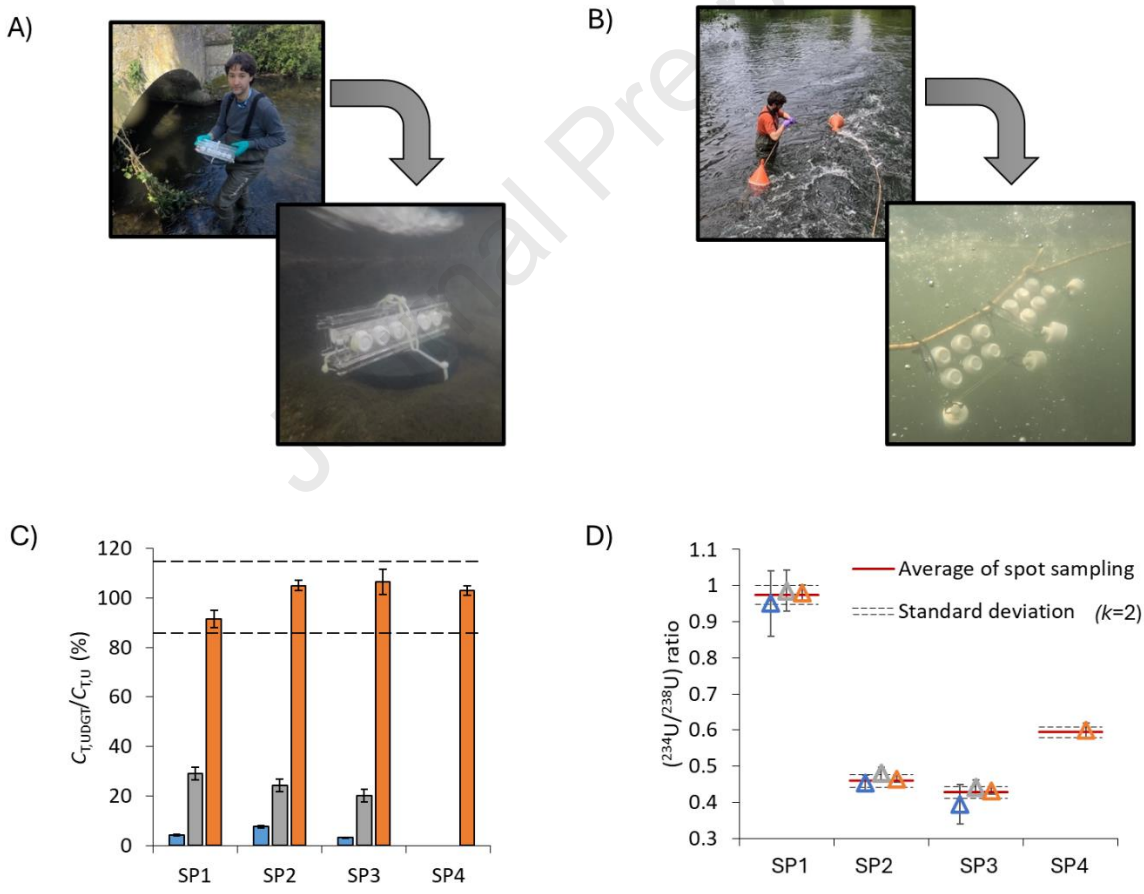

Highlights:

- The new DGT binding material, Monophos, is proposed to measure U concentration.
- A new model for interpreting DGT flux has been developed and tested.
- Ca^{2+}, Mg^{2+} and HCO_3^- interferences were overcome by using the new DGT sampler.
- DGT samplers can trace U sources in waters by means of isotope measurements.

Declaration of interest statements:

The authors declare that they have no known competing financial interests or personal relationships that could have appeared to influence the work reported in this paper.